**NASA TECHNICAL NOTE**

NASA TN D-6797

NASA TN D-6797

# DIFFUSION IN THORIATED AND NONTHORIATED NICKEL AND NICKEL-CHROMIUM ALLOYS AT 1260° C

*by John D. Whittenberger*

*Lewis Research Center*

*Cleveland, Ohio 44135*

NATIONAL AERONAUTICS AND SPACE ADMINISTRATION • WASHINGTON, D. C. • MAY 1972

| 1. Report No.<br>NASA TN D-6797 | 2. Government Accession No. | 3. Reci, |
|---|---|---|
| 4. Title and Subtitle<br>DIFFUSION IN THORIATED AND NONTHORIATED NICKEL AND NICKEL-CHROMIUM ALLOYS AT 1260° C | | 5. Report Date<br>May 1972 |
| | | 6. Performing Organization Code |
| 7. Author(s)<br>John D. Whittenberger | | 8. Performing Organization Report No.<br>E-6748 |
| 9. Performing Organization Name and Address<br>Lewis Research Center<br>National Aeronautics and Space Administration<br>Cleveland, Ohio 44135 | | 10. Work Unit No.<br>114-03 |
| | | 11. Contract or Grant No. |
| 12. Sponsoring Agency Name and Address<br>National Aeronautics and Space Administration<br>Washington, D.C. 20546 | | 13. Type of Report and Period Covered<br>Technical Note |
| | | 14. Sponsoring Agency Code |

15. Supplementary Notes

16. Abstract

Various solid-solid diffusion couples were assembled from thoriated and nonthoriated nickel-base alloys, welded, and diffusion annealed at 1260° C. Concentration profiles indicated that a thoria dispersion does not affect diffusion in Cr(alloy):Ni and Ni-4.8Al:Ni types of couples unless a fine grain structure is retained by the thoria particles. Metallography revealed the presence of thoria-free bands in the thoriated-Ni side of the diffusion zone. The bands contained grain boundaries and, in some cases, non-Kirkendall porosity. A mechanism based on the operation of vacancy sources is proposed to explain the thoria-free bands. In addition, a particular DS-NiCr:Ni couple had negligible Kirkendall porosity. This behavior was related to the grain structure of the particular lot of DS-NiCr.

| 17. Key Words (Suggested by Author(s))<br>Diffusion; Kirkendal porosity; Vacancy sources; TD-Ni; Dispersion-strengthening | 18. Distribution Statement<br>Unclassified - unlimited | | |
|---|---|---|---|
| 19. Security Classif. (of this report)<br>Unclassified | 20. Security Classif. (of this page)<br>Unclassified | 21. No. of Pages<br>42 | 22. Price*<br>$3.00 |

# DIFFUSION IN THORIATED AND NONTHORIATED NICKEL
# AND NICKEL-CHROMIUM ALLOYS AT 1260° C

by John D. Whittenberger

Lewis Research Center

## SUMMARY

In order to compare diffusion in thoriated and nonthoriated nickel-base alloy systems, various solid-solid diffusion couples were assembled, welded, and diffusion annealed at 1260° C. Diffused couples were examined by metallographic, electron microprobe, and, in certain cases, electron replica techniques.

Concentration profiles indicated that a fine thoria ($ThO_2$) dispersion does not affect diffusion in Cr(alloy):Ni and Ni-4.8Al:Ni types of couples unless the particles stabilize a fine grain structure. Metallography, thorium profiles, and electron micrographs of alloy (Co, Cr, Fe, Ni-4.8Al, Ni-20Cr):thoriated nickel couples revealed that thoria-free bands appear in the thoriated nickel side of the diffusion zone. These bands contain grain boundaries and, in some cases, non-Kirkendall porosity. A mechanism based on the operation of vacancy sources is proposed to explain the thoria-free bands. It is concluded that dispersoid-free regions will be formed in a dispersion-strengthened material whenever appreciable diffusion occurs, and regions within the diffusion zone act as net vacancy generators.

Examination of nominally Ni-20Cr:Ni diffusion couples indicated that small silicon additions or silicon-plus-iron additions increase the amount of chromium diffusion and Kirkendall porosity while small manganese additions have no effect. In addition, a particular diffusion couple, DS-NiCr:Ni, exhibited negligible Kirkendall porosity. This behavior is related to the grain structure of the particular lot of DS-NiCr.

## INTRODUCTION

The dispersion-strengthened alloy Ni-20Cr-2$ThO_2$[1] is of current interest for use in

---

[1]All compositions cited in this report are expressed in weight percent.

various high-temperature applications that require high creep strength and good oxidation resistance. For example, thin thoriated Ni-20Cr alloy sheet is currently being considered for part of the thermal protection system of the proposed Space Shuttle (ref. 1). Such alloys are currently being manufactured by two distinct processes. Fansteel, Incorporated, produces sheet, commercially named TD-NiCr, through a combination of powder metallurgy techniques and thermomechanical processing (ref. 2). Sherritt-Gordon Mines, Ltd., produces thin sheet, commercially named DS-NiCr, through the pack chromizing of Ni-2ThO$_2$ sheet (ref. 3).

As a manufacturing process, the pack chromizing method is of interest because of its dependence on chromium diffusion into nickel. The rate of chromium diffusion into nickel essentially determines the maximum thickness of sheet which can economically be produced. In addition, the diffusion of chromium into thoriated nickel disrupts the initial uniform thoria particle distribution. An example of DS-NiCr sheet is shown in figure 1. The light bands are free of thoria particles. In general, the bands are closely associated with grain boundaries parallel to the surface exposed to chromium, and the borders on either side of the bands appear to have been originally mated. No mechanism has been proposed to account for such a structure.

Diffusion in Ni-Cr alloys has been well studied (refs. 4 to 6). In the nickel-rich phase, the interdiffusion coefficient is relatively concentration independent and

$$\tilde{D}(m^2/sec) = 1.25 \times 10^{-4} \exp \frac{-267\ 000\ \text{joules}}{RT} \qquad (1)$$

for 1268 K $\leq$ T $\leq$ 1573 K (ref. 4). In addition, Ugaste (ref. 4) indicated that there was negligible formation of cavities on mutual diffusion in the Ni-Cr system.

The first studies of chromium diffusion into thoriated nickel alloys resulted from attempts to develop an oxidation resistant coating. Fleetwood (ref. 7) plated chromium on a Ni-5ThO$_2$ alloy, which had been produced by mixing, compacting, and extrusion. He annealed couples for various times between 800$^\circ$ and 1150$^\circ$ C. The results indicated that the interdiffusion coefficient of chromium in Ni-5ThO$_2$ was approximately one order of magnitude greater than the interdiffusion chromium in pure nickel over the temperature range studied. He interpreted the "enhanced" diffusion as a result of the stable fine subgrain structure of Ni-ThO$_2$ alloy which allows considerable short-circuit diffusion. In addition, Kirkendall voids were formed on the chromium side of the diffusion couples.

Monson et al. (refs. 8 and 9) pack-chromized and annealed commercial TD-Ni (Fansteel designation for nominal Ni-2ThO$_2$ alloys) sheet to produce a protective alloy layer. Various combinations of time and temperatures, nominally 1090$^\circ$ to 1310$^\circ$ C, were used for both chromizing and annealing. Such treatments apparently did not result

2

in enhanced diffusion since none was reported.  Some porosity near the surface exposed to chromium was observed, generally, for the as-chromized specimens, and the porosity increased with subsequent anneals.  Metallography revealed light colored bands near the chromized surface.  These were approximately parallel to the surface and existed only in the chromium diffusion zone.  The bands could be observed both in the etched and unetched conditions.  The banding occurred regardless of the chromizing conditions or lot of TD-Ni.  Also, the width of the region containing these bands and the width of individual bands increased as the chromizing time increased.  Through electron microprobe analysis and electron replication, it was established that the bands were virtually free of thoria particles.  Furthermore, the individual thoria particle size was the same before and after chromizing, and the thoria-dispersed population (number of particles per unit area) in the chromium concentration gradient, exclusive of the banded regions, was greater than the unaffected TD-Ni.  Thus, it appeared that thoria growth by dissolution of smaller particles did not occur.  The cause of the banded structure was uncertain.

The objectives of this study were to compare diffusion of chromium in various Ni-Cr and Ni-Cr-$ThO_2$ alloys and to examine the formation of the thoria-free bands. Experiments were undertaken to reveal the influence of chemistry and structure on diffusion in thoriated and nonthoriated Ni-Cr alloys.  In addition, the effects of diffusion of iron, cobalt, and aluminum into thoriated nickel alloys were examined.  All studies were conducted at $1260^O$ C.

# EXPERIMENTAL METHODS

Solid-solid diffusion couples were made by pressure welding various alloys together in vacuum at $1150^O$ C for 1 hour.  These were then diffused for 16 hours at $1260^O$ C and rapidly cooled.  Couples were examined by metallographic, electron microprobe, and (in certain instances) electron replication techniques.

## Materials

Table I lists the compositions and forms of the various alloys used to construct diffusion couples.  The nonthoriated alloys had a large-grained equiaxed structure, particularly after being diffusion annealed at $1260^O$ C.  The thoriated alloys had, in general, pancake-shaped grains that were parallel to the sheet surface except for TD-Ni(gs 2)[2], which had a fine-grained equiaxed structure.  Both DS-Ni(gs 1) and DS-NiCr(gs 1) had

---

[2](gs 1) and (gs 2) are being used for identification purposes only.

TABLE I. - COMPOSITION AND FORM OF THE VARIOUS ALLOYS

UTILIZED TO CONSTRUCT DIFFUSION SPECIMENS

| Material | Composition, wt % | Form | Dimension, cm |
|---|---|---|---|
| Ni | Ni-200, nominally 0.25 Mn-0.15 Fe-0.05 Si-0.05 Cu-0.06C- bal Ni | Disk | 1.2 diam by 0.3 |
| Ni(270) | Ni-270, total impurity <208 ppm | Sheet | 2.0 by 2.0 by 0.25 |
| DS-Ni(gs 1) | Nominally Ni-2ThO$_2$ | Sheet | 1.2 by 1.2 by 0.025 |
| DS-Ni(gs 2) | Nominally Ni-2ThO$_2$ | Sheet | 1.2 by 1.2 by 0.037 |
| TD-Ni(gs 1) | Commercial, heat 1596; 2.2 ThO$_2$- other impurity <0.05 - bal Ni | Sheet | 1.2 by 1.2 by 0.31 |
| TD-Ni(gs 2) | Hot extrusion, heat 2977; 2.4ThO$_2$- other impurities <0.02 - bal Ni | Bar | 0.6 by 0.6 by 1.2 |
| Cr | Arc melted | Disk | 1.2 diam 0.3 |
| Ni-20Cr | 19.9Cr-0.4Fe-0.36Mn-1.4Si-0.03C- bal Ni | Sheet | 1.2 by 1.2 by 0.31 |
| Ni-20Cr(pure) | 19.9Cr - bal Ni | Sheet | 1.2 by 1.2 by 0.2 |
| DS-NiCr(gs 1) | Commercial, nominally 21Cr-1.9ThO$_2$- bal Ni (spectrographic analysis indicates trace Fe and Mn) | Sheet | 1.2 by 1.2 by 0.025 |
| DS-NiCr(gs 2) | Commercial, nominally 20Cr-2ThO$_2$- bal Ni (spectrographic analysis indicates trace Fe and Mn) | Sheet | 1.2 by 1.2 by 0.037 |
| TD-NiCr | Commercial, heat 3090; 20.2Cr-2.1ThO$_2$ - other <0.07 - bal Ni (spectrographic analysis indicates trace Co) | Sheet | 1.2 by 1.2 by 0.15 |
| Co | Electrolytic | Sheet | 1.2 by 1.2 by 0.3 |
| Fe | Ingot iron | Disk | 1.2 diam by 0.3 |
| Ni-4.8Al | Ni-4.76Al | Disk | 2.0 diam by 0.2 |
| Ni-20Cr-3Mn | 19.5Cr-2.5Mn - bal Ni | Sheet | 2.0 by 2.0 by 0.2 |
| Ni-20Cr-3Si | 19.9Cr-3.03Si - bal Ni | Sheet | 2.0 by 2.0 by 0.2 |

very-thin elongated pancake-shaped grains about 10 micrometers thick; thus, they possessed very high grain aspect ratios (length/thickness, L/D). Also, DS-Ni(gs-2) and DS-NiCr(gs 2) had high grain aspect ratios, but the grains were much thicker (~100 $\mu$m) than either DS-Ni(gs 1) or DS-NiCr(gs-1). Because of the thinness of the sheet and inability to distinguish individual grains, grain aspect ratios could not be determined for the DS alloys; however, differences are quite obvious in the photomicrographs. The TD-NiCr

4

sheet used in this study had pancake-shaped grains about 50 micrometers thick with a grain aspect ratio of approximately 2.5. The TD-Ni(gs 1) sheet was similar to TD-NiCr. All the DS alloys had much higher grain aspect ratios than the TD alloys.

# PROCEDURE

Typical geometry of the solid-solid diffusion specimens is shown in figure 2. In general, the surfaces to be mated were metallographically polished through 0.05-micrometer alumina. The only exceptions were DS-Ni and DS-NiCr sheet, which were sanded with 600 grit paper only. After the surfaces were prepared, specimens were assembled and welded. Specimens using either DS-Ni or DS-NiCr were constructed with multiple layers of sheet such that their thicknesses in the direction of diffusion was approximately 0.25 centimeter. Table II is a compilation of all the diffusion specimens that were used in this study.

TABLE II. - DIFFUSION SPECIMENS

| Specimen | Components |
|----------|------------|
| 1 | Ni-20Cr:Ni:Cr:Ni-20Cr |
| 2 | Ni-20Cr:DS-Ni(gs 1):Cr:DS-Ni(gs 2):Ni-20Cr |
| 3 | Ni-20Cr:TD-Ni(gs 1):Cr:TD-Ni(gs 2):Ni-20Cr |
| 4 | Ni-20Cr:TD-NiCr:Cr |
| 5 | TD-NiCr:Ni:TD-NiCr |
| 6 | DS-NiCr(gs 1):Ni:DS-NiCr(gs 2) |
| 7 | Fe:TD-Ni(gs 1):Co |
| 8 | Ni:Ni-4.8Al:TD-Ni(gs 2) |
| 9 | DS-Ni(gs 2):Ni-4.8Al:TD-Ni(gs 1) |
| 10 | Ni-20Cr(pure):Ni(270):Ni-20Cr-3Si:Ni(270): Ni-20Cr-3Mn:Ni(270):TD-NiCr |

A vacuum hot press was used to weld all specimens. They were radiantly heated, and molybdenum rams were used to transmit the welding force from a hydraulic press to the specimens. Before welding the molybdenum rams were coated with alumina to promote specimen-ram separation. With one exception all welding was accomplished under a pressure of 21 $MN/m^2$ at $1150^o$ C for 1 hour in a vacuum of $2\times10^5$ torr. The exception was specimen 6 (table II), which was inadvertently welded under a pressure of 104 $MN/m^2$. The higher pressure produced a scattering of small cracks in DS-NiCr (gs 1) and DS-NiCr(gs 2); however, no other detrimental effects were observed.

The as-welded specimens were diffusion annealed in a molybdenum-wound resistance furnace under a flowing ultrapure argon atmosphere at $1260^O$ C. The specimens were slowly heated to approximately $1093^O$ C over several hours, then rapidly heated to $1260^O$ C in half an hour or less. With the exception of the Fe:TD-Ni(gs 1):Co specimen, which was diffused 72 hours, all specimens were diffused 16 hours. After the heat treatment was completed, power to the furnace was cut off, and the furnace cooled to approximately $540^O$ C in 10 minutes. All specimens were extremely clean in appearance after being thus treated. Specimen 2 fractured at one DS-Ni/Cr interface on being removed from the furnace; all other couples were intact.

All diffused specimens were mounted and polished. In general the Cr:thoriated Ni couples were separated at the Cr-rich/Ni-rich phase interface; whether this separation occurred during the diffusion anneal, cool down, or metallographic mounting is not known. Etching was accomplished by one of the following methods: (1) electrolytically through either a chromic acid mixture (100 ml $H_2O$, 10 ml $H_2SO_4$, 2 g chromic acid) or a buffered aqua regia solution (2 parts by volume aqua regia, 1 part glycerine) at 3 to 5 volts; (2) chemically with a swab etch composed of 92 milliliters HCl, 3 milliliters $HNO_3$, and 5 milliliters $H_2SO_4$; (3) a combination of methods (1) and (2). Proper metallographic etching of individual diffusion couples was difficult because of the different materials comprising each specimen. The DS-Ni:Cr couples (specimen 2) were particularly difficult to etch.

After metallography the specimens were repolished and examined in an electron microprobe. Individual diffusion profiles were determined by standard point count techniques and, in some instances, by continuous traverses. The microprobe was operated at 15 kilovolts and a 50-nanoampere specimen current with a beam size of 1 to 2 micrometers; Cr $K_\alpha$ (Fe $K_\alpha$, Co $K_\alpha$, or Al $K_\alpha$ depending on the particular couple), Ni $K_\alpha$, and Th $M_\alpha$ characteristic radiation were continuously monitored and recorded. Point count traverses were made with 2- to 12-micrometer steps, and continuous scans were made at a traversing speed of 10 micrometers per minute.

To determine if any relations exist between microstructure and thoria distribution, portions of certain diffusion couples were bracketed by microhardness indentations. The regions between the indentations were examined by microprobe analysis in 2-micrometer steps. This probe work was performed at 15 kilovolts and a 500-nanoampere beam current with a 1-micrometer spot size; Cr $K_\alpha$ (Fe $K_\alpha$), Ni $K_\beta$ and Th $M_\alpha$ characteristic radiations were monitored and recorded. After probe analysis, each couple in question was etched, and appropriate photomicrographs were taken. Finally, selected couples were examined by electron replica techniques to determine $ThO_2$ distribution and other fine detail.

6

# RESULTS

## Chromium Diffusion in Nickel and Thoriated Nickel Alloys

In figure 3 effective chromium intensity ratio against distance profiles are super-imposed for various Cr:Ni and Ni-20Cr (nominal):Ni types of diffusion couples. The effective chromium intensity ratio $R_{Cr}(X)$ is defined by

$$R_{Cr}(X) = \frac{I_{Cr}(X) - I_{Cr}^{Bkg}}{I_{Cr}^{o} - I_{Cr}^{Bkg}} \tag{2}$$

where $I_{Cr}(X)$ is the intensity of chromium radiation at position X, $I_{Cr}^{o}$ is the intensity of chromium radiation from pure chromium or Ni-Cr alloy, and $I_{Cr}^{Bkg}$ is the intensity (background) of chromium radiation from nickel.

Figures 3(a) and (b) indicate, with two exceptions, that the diffusion of chromium into nickel at 1260° C is not enhanced by the presence of fine thoria particles since the profiles are essentially the same for the various Cr(alloy):Ni(alloy) couples[3]. Both exceptions involve couples with TD-Ni(gs 2) as the chromium sink. Metallography (fig. 4) of these couples indicated that the grain diameter of TD-Ni(gs 2) is approximately 3 micrometers; thus the elongated diffusion zones are probably a result of short circuit diffusion along the grain boundaries. Figure 3(a) also reveals that even though the Cr: thoriated Ni couples may have separated during the diffusion anneal, no noticeable effect on the chromium profiles occurred.

The effect of chemistry on diffusion in nominally Ni-20Cr:Ni types of couples is shown in figure 3(c). For reference a typical profile (TD-NiCr:Ni) from figure 3(b) is replotted in figure 3(c). Several conclusions can be drawn: (1) The diffusion of chromium from a high purity source into a high purity sink is slower than the diffusion of chromium in a relatively impure system (compare Ni-20Cr(pure):Ni(270) with the reference profile); (2) silicon present as an impurity in the chromium source increases the diffusion of chromium into nickel, while manganese as an impurity has little effect (compare Ni-20Cr-3Si:Ni(270) with Ni-20Cr-3Mn:Ni(270)); (3) in pure materials, the presence of fine thoria particles does not affect chromium diffusion (compare TD-NiCr: Ni(270) with Ni-20Cr(pure):Ni(270)); and (4) the presence of chemical impurities in nickel increases subsequent chromium diffusion (compare the reference profile with

---

[3]Actually there should be a very slight difference in measured concentrations when traversing from a nonthoriated alloy to a thoriated alloy due to the presence of approx. 2 percent $ThO_2$ in the thoriated alloy.

TD-NiCr:Ni(270)).

A further indication of the effect of chemistry on diffusion in nominally Ni-20Cr:Ni systems can be seen in figure 5. The amount of Kirkendall porosity formed in the Ni-20Cr(pure):Ni(270) and Ni-20Cr-3Mn:Ni(270) couples is about equal, but these couples have less porosity than either the Ni-20Cr-3Si:Ni(270) or Ni-20Cr:Ni couples. All other things being equal, this difference in Kirkendall porosity would indicate a greater amount of diffusion in the Ni-20Cr-3Si:Ni(270) and Ni-20Cr:Ni systems. With the assumption that the thickness of the diffusion zone is proportional to $\sqrt{Dt}$, an estimate of the effectiveness of small impurity additions on chromium diffusion in nominally Ni-20Cr:Ni couples can be made. From the profiles in figure 3(c) it appears that silicon or silicon-plus-iron additions increase the diffusion coefficient approximately 50 percent at $1260^{U}$ C, that is, $\widetilde{D}$(Si or Si-plus-Fe) = 1.5 $\widetilde{D}$ (unalloyed).

In general it appears that diffusion of chromium into nickel can be influenced by chemical impurities but not simply by the presence of fine thoria particles unless they produce a structure amenable to short-circuit diffusion.

## Thoria-Free Bands

<u>Chromium diffusion</u>. - Although diffusion of chromium in nickel and thoriated Ni alloys appears to be equivalent with respect to the measured chromium diffusion profiles, metallography has revealed the appearance of "whitish" bands in the diffusion zones of Cr(alloy):thoriated Ni alloy couples with the exception of the Cr(alloy):TD-Ni (gs 2) couples. Several examples are shown in figure 6, these are similar to the photomicrograph in figure 1. Again it appears that the bands are associated with grain boundaries that are perpendicular to the direction of diffusion. To determine if the "whitish" bands are merely etching artifacts or truly thoria-free regions, as discussed in the INTRODUCTION, thorium profiles have been established. Figures 7 to 9 are composites of metallography, thorium profiles, and chromium profiles for portions of Cr:TD-Ni(gs 1), Cr:TD-NiCr, and Cr:TD-Ni(gs 2) diffusion couples, respectively. For the sake of comparison, similar data for thoriated Ni-20Cr:Ni couples are shown in figure 10. In this figure, the far left-hand portion of the thorium profile (fig. 10(d)) for the TD-NiCr:Ni couple can be considered to be typical of a normal thoria distribution for any thoriated alloy produced by powder metallurgy techniques. Furthermore, the far right-hand portion of this thorium profile can be considered to be typical of any non-thoriated alloy (i.e., Th background level). In both of these regions only reasonable fluctuations are observed in the thorium profile. On the other hand, the thorium profile (fig. 10(f)) for the DS-NiCr(gs 2):Ni couple exhibits fluctuations in the region of "pure" DS-NiCr to levels which are in the range of the background level. Thus it appears that

certain regions are thoria free. The thorium profile for the DS-NiCr(gs 1):Ni couple (fig. 10(e)) exhibits similar fluctuations to background levels; however, the width of the fluctuations is much narrower than those for the DS-NiCr(gs 2):Ni couple. Examination of the photomicrographs (figs. 10(b)) and (c)) reveals that the "whitish" bands in the DS-NiCr(gs 1) are much narrower than those for the DS-NiCr(gs 2).

In figure 7(c) partial chromium diffusion profiles are superimposed for two widely separated point count traverses of the Cr:TD-Ni(gs 1) diffusion couple. It can be seen that the two chromium profiles agree quite well. The corresponding thorium profiles are plotted in figures 7(b) and (d). Both have fluctuations in the diffusion zone that approach the thorium background level. Figure 7(a) shows the region that corresponds to data from trace 6; again, the "whitish" bands are quite visible.

In figure 8(c) partial diffusion profiles are presented for two widely separated regions of a Cr:TD-NiCr diffusion couple. On the whole, the chromium profiles match well except that there is a chromium-depleted region in trace 12. In figures 8(a) and (b), metallography and a thorium profile corresponding to trace 11 are shown; the large thorium fluctuation centered at 55 micrometers can be associated with the thick "whitish" band in the center of figure 8(a). Figure 8(d) also shows a large thorium fluctuation at 86 micrometers; however, examination of the chromium profile (fig. 8(c)) and metallography (fig. 8(e)) indicates that this fluctuation is due to a void, not to a thoria-free band.

In figure 9, data similar to that presented in figures 7 and 8 are shown for a Cr:TD-Ni(gs 2) couple. Again, the chromium profiles are similar, and thorium fluctuations approaching the background level can be seen, but, no whitish bands can be observed in the photomicrographs.

To examine the thoria particle distribution, the Cr:TD-Ni(gs 1) and Cr:TD-Ni(gs 2) couples were examined by electron replication metallography. In figure 11 a thoria-free zone is shown for the Cr:TD-Ni(gs 1) couple; this band is approximately 120 micrometers from the Cr-rich/Ni-rich phase interface. Note that at least a portion of a grain boundary is visible in the band. Figure 12 shows the typical grain size and thoria distribution for the Cr:TD-Ni(gs 2) couple. The region portrayed is approximately 100 micrometers from the Cr-rich/Ni-rich phase interface. The grain diameter estimate of 1 to 6 micrometers from figure 12 agrees well with the 3 micrometers estimated from figure 4. Figure 12 also reveals that TD-Ni(gs 2) has oversized thoria particles that are generally in the grain boundaries. Such an arrangement would lead to large fluctuations in the thorium profiles (fig. 9).

Diffusion of other substitutional atoms. - It appears that the diffusion of chromium into thoriated nickel alloys disrupts the generally uniform thoria distribution. To see if the diffusion of other substitutional atoms into thoriated Ni alloys would produce similar effects, Fe:TD-Ni(gs 1), Co:TD-Ni(gs 1), and Ni-4.8Al:thoriated Ni couples were

assembled, welded, and diffused at 1260° C. Iron and cobalt were chosen because of
(1) large solubility in nickel, (2) ability to be exposed to 1260° C, and (3) differences in
diffusion coefficients in the nickel-rich phase (ref. 10). The alloy Ni-4.8Al was chosen
because Monson et al. (refs. 8 and 9) did not observe thoria-free zones after pack alu-
minizing and annealing TD-Ni sheet. Photomicrographs of typical cross sections of the
diffused couples are shown in figure 13. A banded structure similar to that previously
observed can be readily seen in the Fe:TD-Ni(gs 1) and the Co:TD-Ni(gs 1) couples. It
also appears that the Ni-4.8Al:thoriated Ni couples have whitish bands in the diffusion
zone; however, they are very narrow and are difficult to reveal.

Figure 14 is a composite of metallography, partial thorium profiles, and partial
iron profiles for the Fe:TD-Ni(gs 1) couple. The iron profiles are in good agreement,
and the thorium profiles reveal that wide thoria-free regions exist. Again, comparison
of the metallography with the thorium profiles indicates that the "whitish" bands are
free of thoria. In addition, the thorium profiles indicate that thoria-free zones are not
confined to specific compositions such as the marker plane in most binary diffusion
couples. Further confirmation of the thoria distribution can be seen in the electron-
photomicrograph shown in figure 15.

A continuous electron microprobe traverse of the Co:TD-Ni(gs 1) couple is plotted
in figure 16. Several fluctuations to background level are evident in the thorium tra-
verse; thus, the whitish bands in figure 13(b) are free of thoria. This conclusion is
reinforced by the electron photomicrographs shown in figure 17. Figures 17(a) and (b)
are approximately 105 and 135 micrometers (positions B and C, fig. 16), respectively,
from the original interface (position A, fig. 16); thus, both bands are well within the
diffusion zone. These photomicrographs indicate that there is a close connection be-
tween the appearance of thoria-free zones, grain boundaries, and the direction of diffu-
sion. Figure 17(b) is especially interesting since a thoria-free region is not formed
along a small length of grain boundary that is parallel to the direction of diffusion.
These photomicrographs are typical examples of thoria-free zones found in the Co:TD-
Ni(gs 1) couple. In all instances the thoria-free zones contained grain boundaries. Fig-
ure 17(c) contains a grain boundary approximately 270 micrometers (position D, fig. 16)
from the original interface (position A, fig. 16). For all practical purposes this grain
boundary lies outside the diffusion zone, and a thoria-free band has not been formed.

In figure 18 the effective aluminum intensity ratio $R_{Al}(X)$ against distance profiles
for various Ni-4.8Al:Ni alloy couples are superimposed where $R_{Al}(X)$ is defined by
equation (2) with aluminum substituted for chromium. This figure again indicates the
equivalence of bulk diffusion in thoriated and nonthoriated systems, since all profiles,
with the exception of the Ni-4.8Al:TD-Ni(gs 2) couple, are equivalent. As was the case
for chromium diffusion in TD-Ni(gs 2), the elongated diffusion zone in the Ni-4.8Al:TD-
Ni(gs 2) couple is probably due to short-circuit diffusion along grain boundaries. Par-
tial thorium and aluminum profiles are plotted for the Ni-4.8Al:TD-Ni(gs 1) couple in

10

figure 19. From the thorium profile alone it is not evident that thoria-free bands were formed; on the other hand, figure 20 definitely shows a thoria-free zone and associated grain boundary. Similar results were obtained for the Ni-4.8Al:DS-Ni(gs 2) couple.

## Void Formation

Non-Kirkendall porosity. - Re-examination of figures 1, 6(c), 6(d), 8(a), and 8(e) reveals that several diffusion couples contain voids that are not normal Kirkendall voids; that is, this porosity was formed in the neighborhood of the slower moving specie, while Kirkendall voids form in the neighborhood of the faster specie. In all cases these non-Kirkendall voids were (1) within the diffusion zone, (2) attached to grain boundaries, and (3) at least partially contained within thoria-free bands. In general the voids have a semicircular cross section; however, in many instances several pores have impinged forming narrow elongated shapes.

Kirkendall porosity. - Nonthoriated alloys: As indicated in the chromium diffusion section, small alloy additions to nominally Ni-20Cr can influence the rate of diffusion and apparently the amount of Kirkendall porosity. With a Ni-20Cr(pure):Ni(270) couple as reference, small additions of silicon or silicon-plus-iron increase the amount of Kirkendall porosity while small manganese additions have no effect (fig. 5).

Thoriated alloy: Data for nominally Ni-20Cr-2ThO$_2$:Ni diffusion couples are presented in figure 10. In addition to showing the equivalence of the chromium profiles, this figure reveals a difference in Kirkendall void formation. Both the TD-NiCr:Ni and the DS-NiCr(gs 2):Ni couples have considerable Kirkendall porosity, but the DS-NiCr(gs 1): Ni couple has essentially no porosity (the few pits in fig. 10(b) are believed to be cracks that have rounded during the diffusion anneal).

## DISCUSSION

In the previous section several interesting phenomena were observed to accompany diffusion: (1) the formation of thoria-free zones, (2) non-Kirkendall porosity, and (3) the absence of Kirkendall porosity in the DS-NiCr(gs 1):Ni diffusion couple. Additionally, it was revealed that the rate of diffusion in nickel-rich phase of the Ni-Cr system depends on the type and amount of impurity elements, but the rate is not affected by the presence of thoria particles unless they retain a structure amenable to short-circuit diffusion. Thus, diffusion information obtained in nonthoriated Ni-Cr systems can, in general, be applied to thoriated Ni-Cr systems. Similar comments also apply for diffusion in the nickel-rich Ni-Al solid solution. Such results indicate that diffusion in any

nickel-rich substitutional solid solution is probably not affected by a fine thoria particle dispersion unless a short-circuit diffusion structure is stabilized.

## Thoria-Free Zones and Non-Kirkendall Porosity

Experimental observations. - Briefly, the experimental observations concerning thoria-free zones and non-Kirkendall porosity are as follows:

(1) Thoria-free bands are formed during the diffusion of chromium, cobalt, iron, and aluminum into thoriated nickel alloys at $1260^\circ$ C.

(2) The thoria-free bands are generally perpendicular to the direction of diffusion.

(3) The thoria-free bands contain grain boundaries.

(4) In many instances the borders of the thoria-free zones appear to have been originally mated.

(5) Thoria-free zones are not restricted to specific compositions.

(6) In some cases non-Kirkendall voids are formed in the neighborhood of the slower moving nickel. These voids are contained within thoria-free zones and are attached to grain boundaries.

In addition Monson et al. (refs. 8 and 9) observed the following during pack chromizing of TD-Ni sheet:

(7) Thoria-free bands formed during chromium diffusion into TD-Ni sheet between $1090^\circ$ and $1310^\circ$ C.

(8) The width of the region containing thoria-free bands and the width of individual bands increased as the chromizing time increased.

(9) The individual thoria particle size was about the same before and after chromizing.

Possible mechanisms. - Considering the formation of thoria-free zones only, there are several possible mechanisms for moving (removing) thoria particles:

(1) Dissolution

(2) Reduction by impurities during diffusion

(3) Sweeping by moving grain boundaries

(4) Sweeping along grain boundaries

(5) Operation of vacancy sources.

In the dissolution mechanism, thoria particles would simply dissolve. This mechanism would be a function of temperature and reactivity of the alloy matrix. In general, such a mechanism would operate anywhere in the alloy; thus, it appears unreasonable to expect thoria-free bands to form only in the diffusion zone. Additionally, the distribution of individual thoria particles and median particle diameter in TD-Ni sheet were unchanged after 200-hour anneals from $100^\circ$ to $1400^\circ$ C (ref. 11), and very slight, if

any, thoria particle size increase was observed when TD-Ni, TD-NiCr, and DS-NiCr were annealed 2000 hours at $1090^{\circ}$ C (refs. 12 and 13). These observations indicate that thoria particles are inert, and the dissolution mechanism is inactive.

Another possible mechanism would involve the selective reduction of thoria particles by impurity atoms during diffusion. The metallic thorium could diffuse sway and reoxidize elsewhere. This mechanism would operate in the diffusion zone, but it is difficult to imagine thoria-free bands appearing. Thermodynamically for chromium, aluminum, and iron diffusion, the following reactions must take place:

$$3ThO_2 + 4Cr \rightarrow 2Cr_2O_3 + 3Th \qquad (3)$$

$$3ThO_2 + 4Al \rightarrow 2Al_2O_3 + 3Th \qquad (4)$$

$$ThO_2 + 2Fe \rightarrow 2FeO + Th \qquad (5)$$
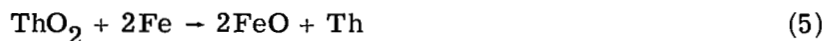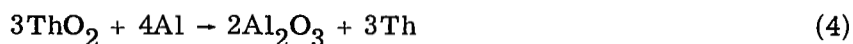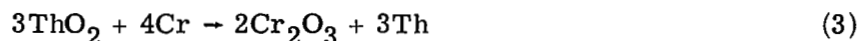
From data in references 14 and 15, the standard free energies of formation at $1260^{\circ}$ C were calculated to be 1.84, 1.25, and 0.29 megajoules for equations (3) to (5), respectively; therefore, they are improbable. Similar reactions for cobalt and nickel with thoria are equally improbable. In addition, Monson et al. (refs. 8 and 9) observed that the thoria particle size in TD-Ni sheet was not affected by pack chromizing or pack chromizing plus annealing between $1090^{\circ}$ and $1310^{\circ}$ C. Also, Chang (ref. 16) observed no change in thoria particle size after pack aluminizing TD-NiCr sheet for 4 hours at $1090^{\circ}$ C and annealing 200 hours at $1260^{\circ}$ C. These points negate the reduction during diffusion mechanism.

A mechanism that can account for a banded structure involves the concept that thoria-free zones are formed by moving grain boundaries that sweep particles. If this mechanism were active, thoria-free bands should be formed any time grain boundaries move; for example, during recrystallization. This simply has not been observed for either TD-NiCr or TD-Ni (refs. 17 to 19). The grain-boundary sweep mechanism can be restricted to be operative only when assisted by diffusion. However, examination of thoria-free zones by electron replica techniques have not detected any unusual thoria agglomerations on or near the grain boundaries associated with thoria-free bands (refs. 8 and 9; figs. 15, 17, and 20). The grain boundary sweeping mechanism does not appear to be operating.

The sweeping of thoria particles down grain boundaries is another possible mechanism. As above, it must operate only when assisted in some manner by the diffusive flux since thoria-free zones were not formed during simple annealing (ref. 11). Even with this restriction, sweeping down grain boundaries is probably not operative since no unusual agglomerations of thoria have been seen.

Proposed mechanism. - I believe the formation of thoria-free bands to be a direct result of the vacancy-exchange mechanism of diffusion. Just as Kirkendall porosity offers visual proof that vacancy sinks are active in a diffusion couple, the thoria-free bands are visual proof that vacancy sources are also active in a diffusion couple. The thoria particles do not take part in the diffusion process; they are simply inert markers that allow the observation of net mass transport.

In the couples studies, diffusion apparently occurred by the vacancy mechanism, for Kirkendall porosity is evident in most couples (figs. 5, 10, and 13). Since diffusion by the vacancy mechanism is considered to occur by an exchange in positions between an atom and a neighboring vacancy, the result of substitutional diffusion in a thoriated alloy should be an increased interparticle spacing due to dilution of the original thoriated alloy matrix. Thus, thoria-free bands should not appear. However, if the grain boundaries on the thoriated alloy side of the diffusion couple act as vacancy sources, it is possible for a banded structure to form. In order for a grain boundary (or, for that matter, any region) to act as a vacancy generator, it must absorb a number of atoms equal to the number of vacancies created. Down-climb of an edge dislocation is a simple vacancy generation process. To increase the depth of the extra half-plane of atoms (fig. 21(a)), a vacancy is created in the existing lattice when an atom jumps from a lattice site to the half-plane (fig. 21(b)). Thus, matter is added to the vicinity of a vacancy source.

Considering diffusion on the side of a couple where vacancy sources are active, matrix atoms, substitutional impurity atoms, and vacancies would be continuously passing through the grain boundaries. If the boundary acts as a source of vacancies (more vacancies leave than are absorbed), a net increase of material in the region of the boundary must occur. On examination of an ordinary diffusion couple, nothing unusual would be seen in the microstructure since the grain boundaries are not marked. On the other hand, in a diffusion couple containing a thoriated alloy, grain boundaries are well marked by thoria particles (fig. 17(c)). During diffusion, a mass of material necessary to compensate for the net production of vacancies would be absorbed at the grain boundary. This material essentially pushes the thoria particles on either side of the boundary apart resulting in the mated appearance of the band borders (fig. 1). Once a thoria-free band is started, the grain boundary probably moves within the band except for points that were originally pinned by thoria particles. The extent and direction of movement is most likely regulated by the diffusion fluxes and the tendency for grain growth.

In general, thoria-free bands should be roughly perpendicular to the direction of diffusion and parallel to each other since the diffusion couple can easily expand in this direction. If thoria-free bands were formed parallel to the direction of diffusion, the diffusion couple would bend in order to accommodate the additional material; however, the geometry of a unidimensional diffusion couple generally prohibits such bending. The

14

number of bands formed would depend on the original grain structure of the thoriated alloy. Additionally, the region in which the bands appear and the width of individual bands will increase as the amount of diffusion is increased.

Inherent in this discussion is the assumption that vacancy sources are active in the thoriated side of the diffusion couple. This is only the case when the impurity atom entering the thoriated alloy diffuse at a faster rate than the matrix atom; that is, the intrinsic diffusion coefficient of the impurity atom (Al, Co, Cr, or Fe) is greater than the intrinsic diffusion coefficient of the matrix atom (Ni). This insures that the net flux of vacancies is toward the impurity atom source. For the reverse case (thoriated alloy contains the faster-moving component), Kirkendall porosity, not thoria-free bands, would form on the thoriated side of the diffusion couple. This was observed for TD-NiCr:Ni diffusion couple (fig. 10(a)). Obviously for a binary diffusion couple composed of two thoriated alloys, thoria-free bands would appear on one side of the diffusion zone and Kirkendall porosity on the other. The only exception being the special case where the intrinsic diffusion coefficients of both species are equal.

The appearance of non-Kirkendall porosity in the thoria-free bands of several diffusion couples is probably due to the inability of the hard thoriated alloy to remain integral with the softer thoria-free material. During diffusion, stresses are established due to the net transport of mass. It is possible that the stress conditions are such that a small crack can develop at a grain boundary in the nonthoriated alloy. Once a crack is formed, it can grow because of the continuous flow of vacancies into it.

Other observations. - The experimental data developed for the various diffusion couples seem to indicate that the banded structure formed during diffusion in thoriated nickel alloys would be found in most alloy systems if they were properly marked; that is, contain a fine dispersion of inert particles. The bands would be formed at grain boundaries (vacancy sources) in the neighborhood of the slower-moving specie and, in general, should be more readily observable for couples that had extensive Kirkendall porosity.

Finally, for certain cases, it is possible for dispersoid-free bands to form due to self-diffusion. An example of this would be solid-state welding of dispersion-strengthened alloys where a dispersoid-free band is formed at the weld line due to the elimination of pores entrapped due to welding. This has been observed during solid-state welding of TD-Ni (ref. 20) and TD-NiCr (ref. 21).

With regard to thoriated alloys produced by metallizing and annealing (DS-NiCr process), the final structure will consist of a three-dimensional network of thoria-free material separating thoriated regions. The intricacy of the network will depend on the original grain structure of the thoriated alloy to be metallized and the amount of diffusion seen by each grain boundary. The effect of such a structure on mechanical properties is unknown.

# Kirkendall Porosity

In figure 10 there is a significant difference in the Kirkendall porosity found in essentially equivalent diffusion couples. Because of the similarity of the chromium diffusion profiles, the difference in porosity is probably not due to impurity content. Therefore, the absence of porosity in the DS-NiCr(gs 1):Ni couple must be structure related.

Kirkendall voids are thought to form on the side of the faster moving specie because of either (1) existance of large nuclei such as imperfections, voids, or impurities, or (2) a two-dimensional tensile stress produced by the net loss of atoms (refs. 22 and 23). If imperfections alone are required to form Kirkendall porosity, no differences should be detected between various thoriated Ni-20Cr:Ni couples. On the other hand, if a tensile stress, in possible combination with existing imperfections, is required to produce voids, it may be possible for DS-NiCr(gs 1) to avoid pore formation.

Brinkman (ref. 23) has shown that a two-dimensional tensile stress is established in a solid-solid diffusion couple on the side suffering a net loss of atoms. This stress field is supposedly due to the annihilation of vacancies on edge dislocations whose Burger's vectors are not perpendicular to the Kirkendall interface. For the special case where vacancy annihilation occurs predominately on edge dislocations with Burger's vectors perpendicular to the Kirkendall interface, no stress field would be established since relaxation is permitted in the direction of diffusion. Thus, pores would not be formed.

Examination of the DS-NiCr(gs 1):Ni couple (fig. 10(b)) reveals that considerable grain boundary area parallel to the Kirkendall interface exists on the chromium rich side of the couple. This is due to the high grain aspect ratio and small grain width (high L/D with small D) of DS-NiCr(gs 1). It is felt that vacancy annihilation at such boundaries is similar to annihilation at edge dislocations with Burger's vectors perpendicular to the Kirkendall interface. Such behavior results in contraction only in the direction of diffusion (stress fields are not established).

The study of thoriated Ni-Cr:Ni diffusion couples can be useful to predict the oxidation behavior of the thoriated alloy. Couples simulate the case where oxidation is controlled by the diffusion of chromium to the surface. Data obtained in this study indicate that large grain size Ni-20Cr-2ThO$_2$ alloys are susceptible to Kirkendall porosity. Such void formation is important when considering the ultimate load-bearing capacity of thoriated alloy sheet envisioned as part of the thermal protection system for the Space Shuttle. Recent static and dynamic oxidation tests of DS-NiCr and TD-NiCr sheet (refs. 24 and 25) have confirmed the results of these diffusion studies.

16

# SUMMARY OF RESULTS

Based on a study of diffusion couples constructed from various thoriated and non-thoriated nickel-base alloys and diffusion annealed at $1260^{\circ}$ C, the following results were obtained:

(1) Thoria-free bands formed during the diffusion of chromium, iron, cobalt, and aluminum into thoriated nickel alloys. In all cases the thoria-free bands were found at grain boundaries within the diffusion zone. In addition certain diffusion couples contained non-Kirkendall porosity within the thoria-free bands.

(2) The formation of thoria-free bands and non-Kirkendall porosity was dependent on the amount and direction of diffusion and the grain structure of the thoriated alloy.

(3) All nominally Ni-20Cr:Ni diffusion couples exhibited Kirkendall porosity with the exception of a particular DS-NiCr:Ni couple, which was constructed with a fine-grained (high L/D with small D) DS-NiCr.

(4) The presence of a fine thoria dispersion did not enhance diffusion unless the particles stabilized a short-circuit diffusion structure, that is, a fine grain size.

(5) Small silicon or silicon-plus-iron additions to nominally Ni-20Cr increased the rate of chromium diffusion in Ni-20Cr:Ni couples, but small manganese additions had no effect.

# CONCLUSIONS

From the results obtained during a study of binary diffusion in thoriated and non-thoriated nickel-base alloys at $1260^{\circ}$ C, the following conclusions are drawn:

1. Dispersoid-free regions will appear in a dispersion strengthened material wherever appreciable diffusion occurs and regions within the diffusion zone act as net vacancy generators.

2. The ability of a fine grained (high L/D with small D) DS-NiCr to exhibit negligible Kirkendall porosity in a diffusion couple is related to the grain structure that absorbs vacancies and allows contraction only in the direction of diffusion.

3. The presence of an inert dispersoid in an alloy matrix will not, in itself, lead to enhanced diffusion unless a short-circuit diffusion structure is stabilized.

Lewis Research Center,
    National Aeronautics and Space Administration,
        Cleveland, Ohio, March 1, 1972,
            114-03.

# REFERENCES

1. Saunders, Neal T.: Dispersion-Strengthened Alloys for Space Shuttle Heat Shields. Space Transportation System Technology Symposium. Vol. III - Structures and Materials. NASA TM X-52876, 1970, pp. 159-174.

2. Klingler, L. J.; and Weinberger, R.: Production of Dispersion Strengthened Nickel-Chromium Alloys. Presented at the SAMPE Space Shuttle Materials Conference, Madison, Ala., Oct. 5-7, 1971.

3. Fraser, Robert W.; Kuschnir, Bud W.; and Weizenbach, Bauke: Method of Producing Dispersioned Strengthened Nickel Chromium Alloys. U.S. Patent 3,454,431, July 22, 1966.

4. Ugaste, Yu. E.: Mutual Diffusion in the System Ni-Cr. Phys. Metals Metallography, vol. 24, no. 3, 1967, pp. 57-65.

5. Monma, K.; Suto, H.; and Oikawa, H.: Diffusion of $Ni^{63}$ and $Cr^{51}$ in Nickel-Chromium Alloys (On the Relation between High-Temperature Creep and Diffusion in Nickel Base Solid Solutions, I). J. Japan Inst. Metals, vol. 28, 1964, pp. 188-192.

6. Heumann, Th.; and Reerink, W.: Measurement of the Isotope Effect for Diffusion in the System Chromium-Nickel by Means of a Mass Spectrometric Analysis. Acta Met., vol. 14, no. 2, Feb. 1966, pp. 201-207.

7. Fleetwood, M. J.: The Diffusion of Chromium into Nickel-Thoria Alloys. J. Inst. Metals, vol. 94, 1966, pp. 218-223.

8. Monson, L. A.: Protective Coatings for Dispersion-Strengthened Nickel. Oxide Dispersion Strengthening. G. S. Ansell, T. D. Cooper, and T. V. Lenel, eds., Gordon and Breach, Science Publ., 1968, pp. 563-607.

9. Monson, L. A.; and Pollock, W. I.: Development of Coatings for Protection of Dispersion Strengthened Nickel from Oxidation. Part 1. Oxidation Studies, Coating Development and Coating Analysis. E. I. du Pont de Nemours and Co., Inc. (AFML-TR-66-47, pt. 1, AD-808519), Mar. 1966.

10. Wohlbier, F. H., ed.: Diffusion Data. Vol. 4, 1970, pp. 21, 35.

11. Inman, M. C.; and Smith, P. J.: An Electron Transmission Study of Oxide Particle Statistics in TD Nickel Alloy. Oxide Dispersion Strengthening. G. S. Ansell, T. D. Cooper, and F. V. Lenel, eds., Gordon and Breach, Science Publ., 1968, pp. 291-321.

12. Sims, Chester T.: Structural Stability in $Ni-2ThO_2$ Alloy. Trans. AIME, vol. 227, no. 6, Dec. 1963, pp. 1455-1457.

13. Sims, C.: Visual Observations on Thoria Dispersions in Nickel Alloys. Oxide Dispersion Strengthening. G. S. Ansell, T. D. Cooper, and F. V. Lenel, eds., Gordon and Breach, Science Publ., 1968, pp. 489-493.

14. Peterson, Sigfred; and Curtis, C. E.: Thorium Ceramics Data Manual. Vol. 1: Oxides. Rep. ORNL-4503, vol. 1, Oak Ridge National Lab., Sept. 1970, p. 5.

15. Darken, Laurence S.; and Gurry, Robert W.: Physical Chemistry of Metals. McGraw-Hill Book Co., Inc., 1953, p. 349.

16. Chang, W. H.: Some Observations of the Effect of Aluminum on Thoria Agglomeration in a Ni-20%Cr Alloy. Trans. ASM, vol. 60, no. 4, Dec. 1967, pp. 730-732.

17. Arnold, D. B.; and Klingler, L. J., Jr.: Dispersion-Strengthened Nickel Base Alloys. Oxide Dispersion Strengthening. G. S. Ansell, T. D. Cooper, and F. V. Lenel, eds., Gordon and Breach, Science Publ., 1968, pp. 611-635.

18. Kimmel, E. R.; and Inman, M. C.: Recrystallization in Thoria-Dispersion Nickel Sheet. Trans. ASM, vol. 62, no. 2, June 1969, pp. 390-397.

19. Webster, D.: Grain Growth and Recrystallization in Thoria-Dispersion Nickel and Nichrome. Trans. AIME, vol. 242, no. 4, Apr. 1968, pp. 640-648.

20. Moore, Thomas J.; and Holko, Kenneth H.: Solid-State Welding of TD-Nickel Bar. NASA TN D-5918, 1970.

21. Holko, Kenneth H.; and Moore, Thomas J.: Enhanced Diffusion-Welding of TD-NiCr Sheet. NASA TN D-6493, 1971.

22. Seitz, F.: On the Porosity Observed in the Kirkendall Effect. Acta Met., vol. 1, May 1953, pp. 355-369.

23. Brinkman, J. A.: Mechanism of Pore Formation Associated with the Kirkendall Effect. Acta Met., vol. 3, Mar. 1955, pp. 140-145.

24. Sanders, W. A.; and Barrett, C. A.: Oxidation Screening at $1204^O$ C ($2200^O$ F) of Candidate Alloys for the Space Shuttle Thermal Protection System. Presented at the SAMPE Space Shuttle Materials Conference, Madison, Ala., Oct. 5-7, 1971 (NASA TM X-67864).

25. Giggins, C. S.; and Pettit, F. S.: The Oxidation of TD NiC(Ni-20Cr-2 vol pct $ThO_2$) between $900^O$ and $1200^O$ C. Met. Trans., vol. 2, no. 4, Apr. 1971, pp. 1071-1078.
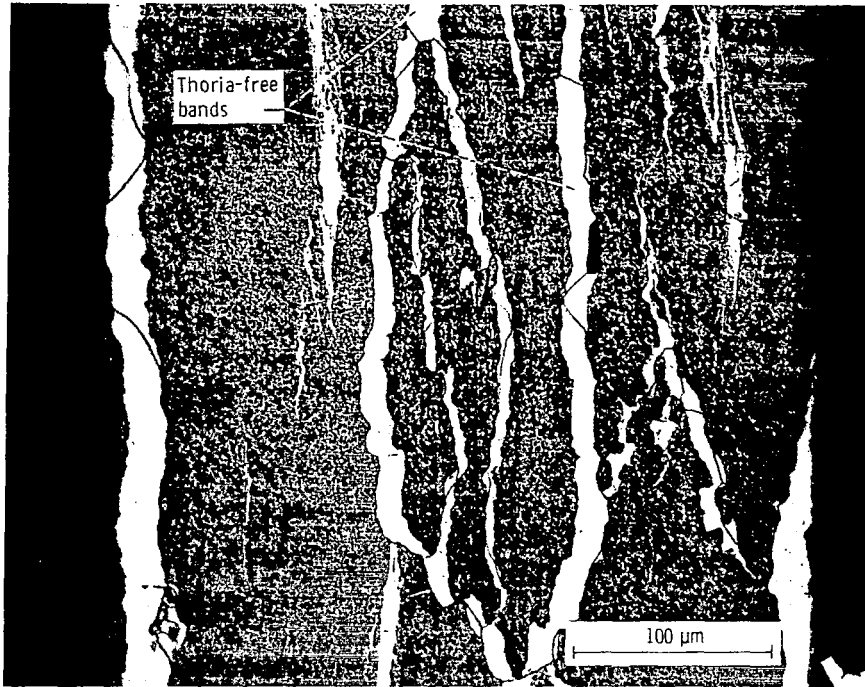
Figure 1. – Photomicrograph of DS-NiCr (nominally Ni-20Cr-2ThO$_2$) sheet produced by pack chromizing DS-Ni (nominally Ni-2ThO$_2$). Electrolytically etched with chromic acid mixture.
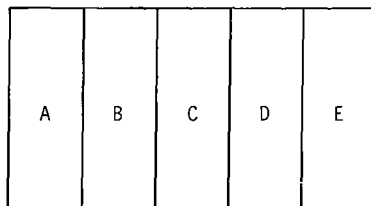


Figure 2. – Schematic drawing of typical solid-solid diffusion specimen. In general A, B, C, D, and E are different alloys; thus, data on four separate diffusion couples are obtained.
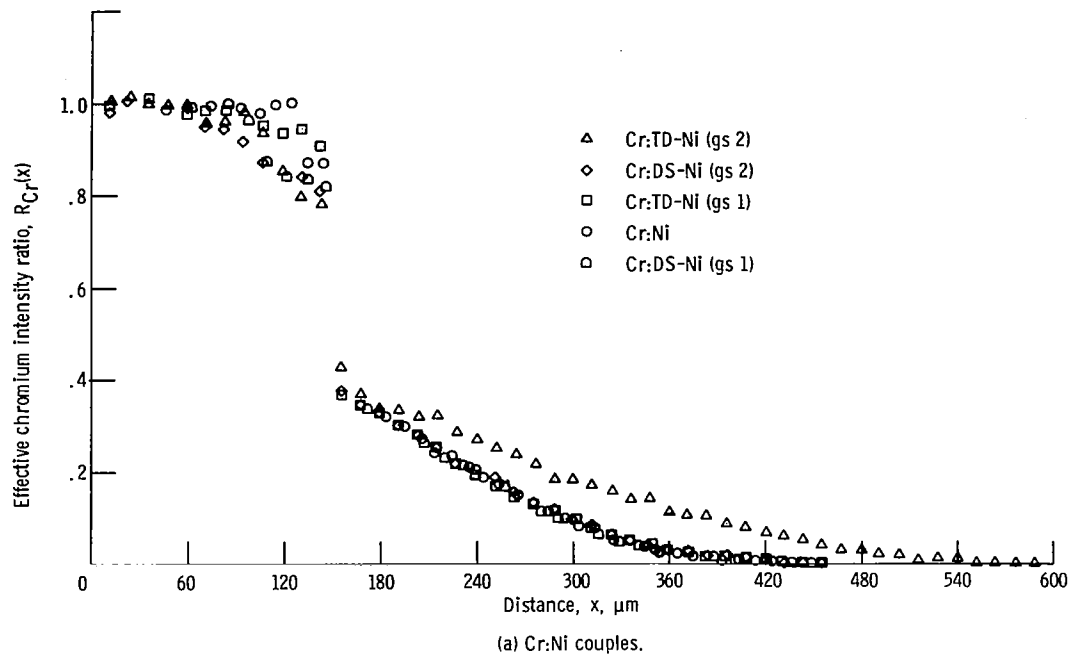
Figure 3. - Effective chromium intensity ratio as function of distance for various diffusion couples. All couples diffused 16 hours at 1260° C in argon.

(a) Cr:Ni couples.

(b) Ni-20Cr (nominal):Ni couples.

(c) Ni-20Cr-X:Ni couples.
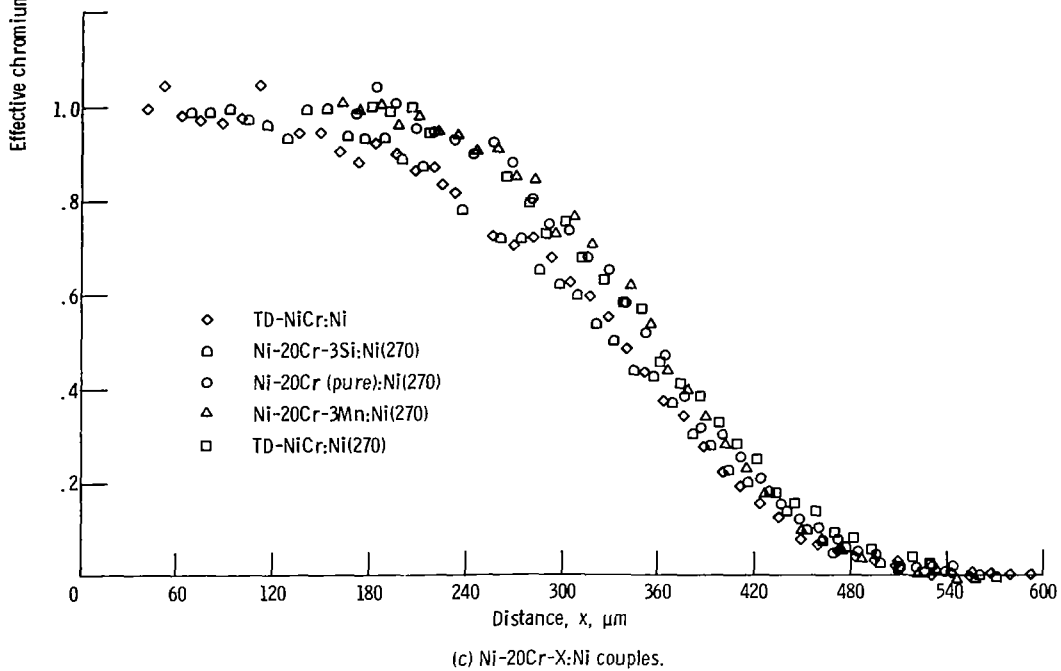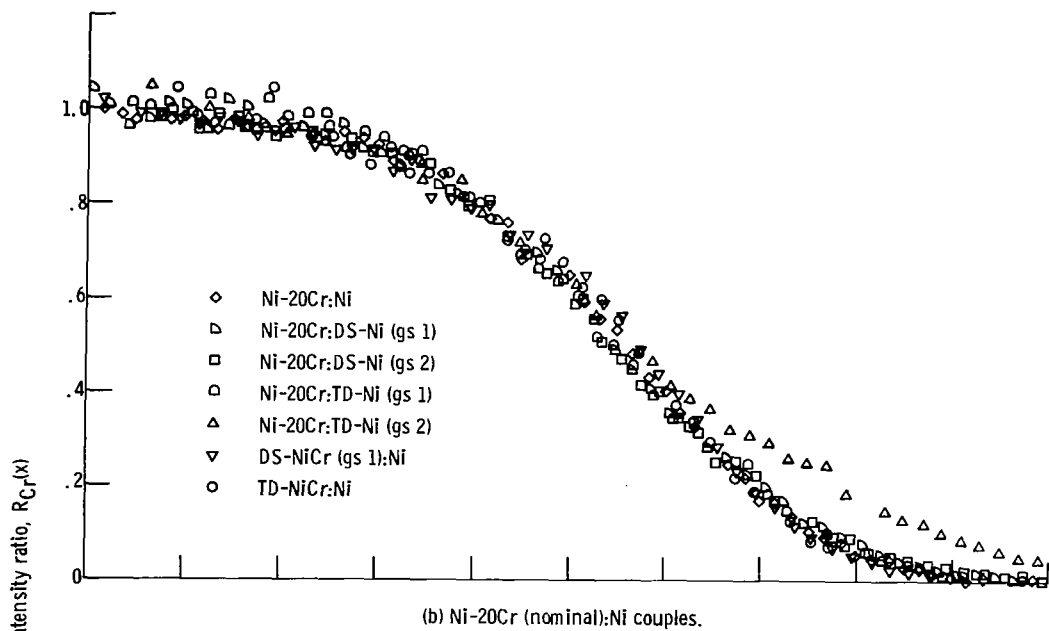
Figure 3. – Concluded.
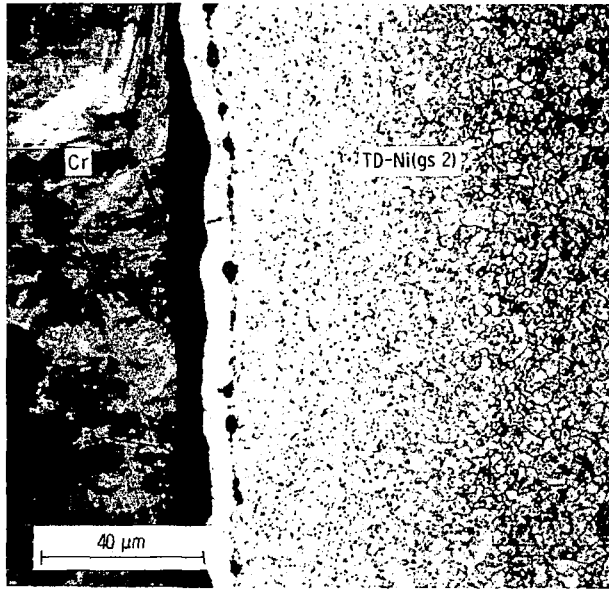
(a) Cr:TD-Ni(gs 2).
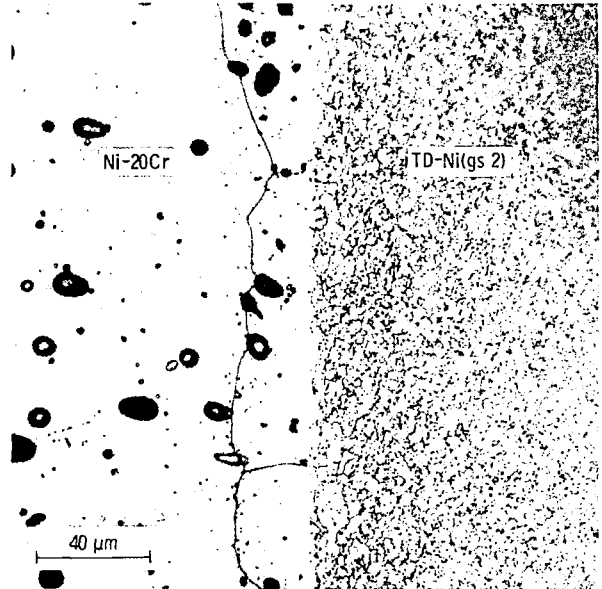
(b) Ni-20Cr:TD-Ni(gs 2).

Figure 4. - Photomicrographs of Cr(alloy):TD-Ni(gs 2) couples diffused 16 hours at $1260^0$ C in argon. Electrolytically etched with chromic acid mixture.

(a) Ni-20Cr(pure):Ni(270).

(b) Ni-20Cr-3Mn:Ni(270).

(c) Ni-20Cr-3Si:Ni(270).
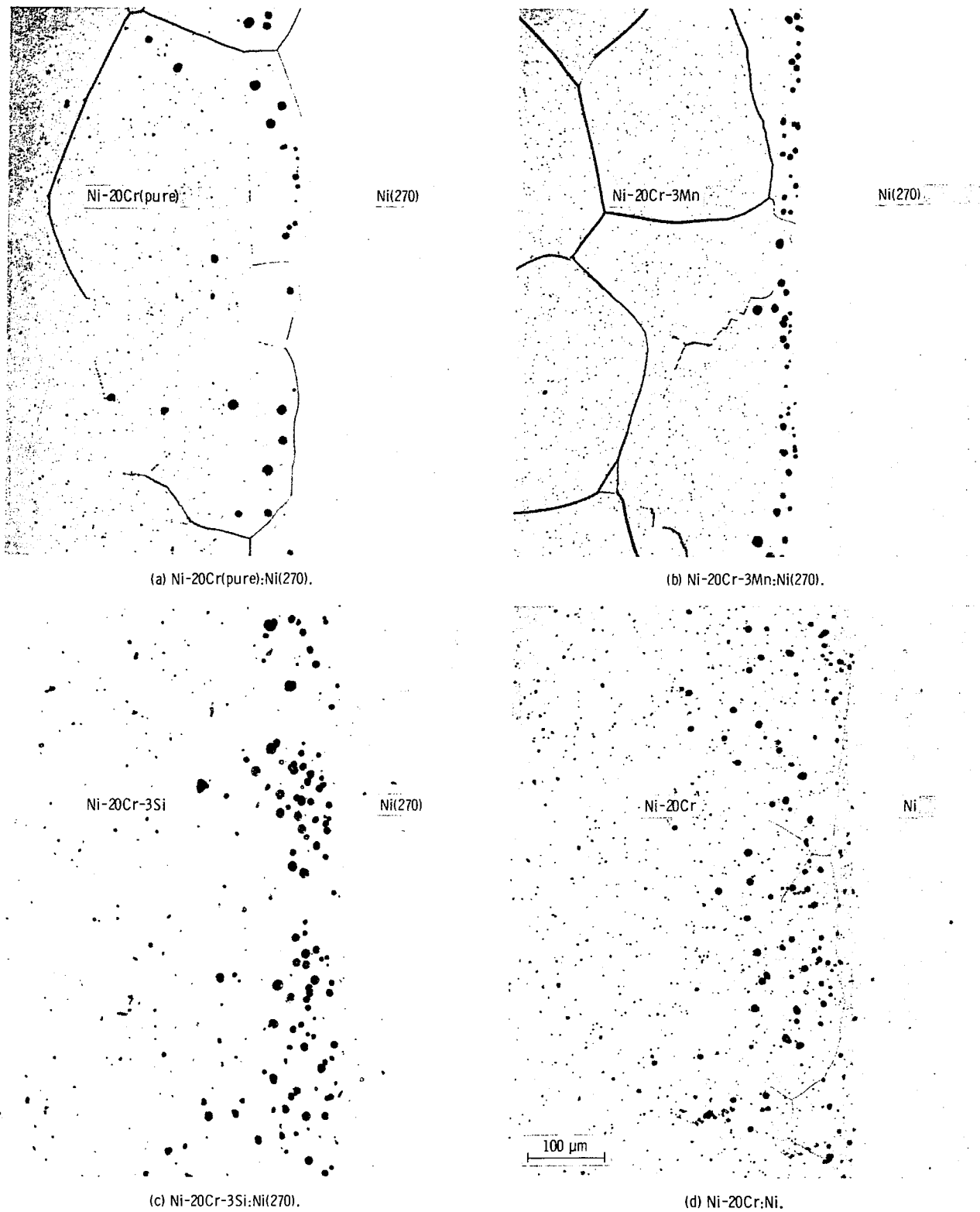
(d) Ni-20Cr:Ni.

Figure 5. - Photomicrographs of various Ni-20Cr:Ni couples diffused 16 hours at 1260° C in argon. Electrolytically etched with chromic acid mixture.

24
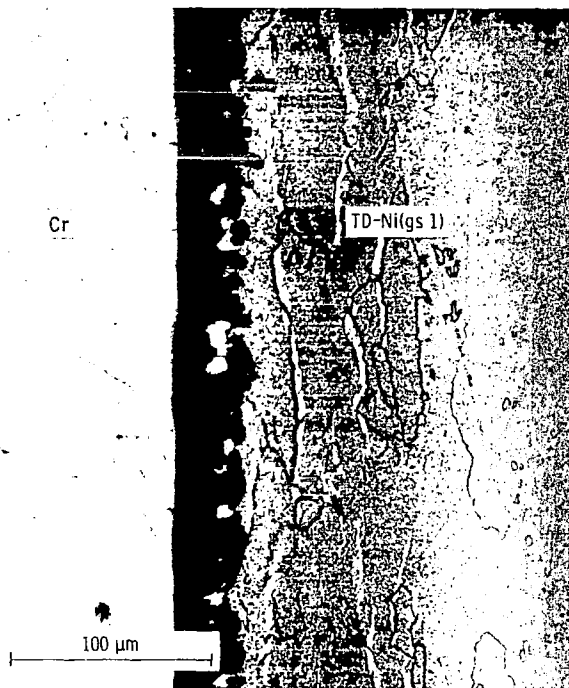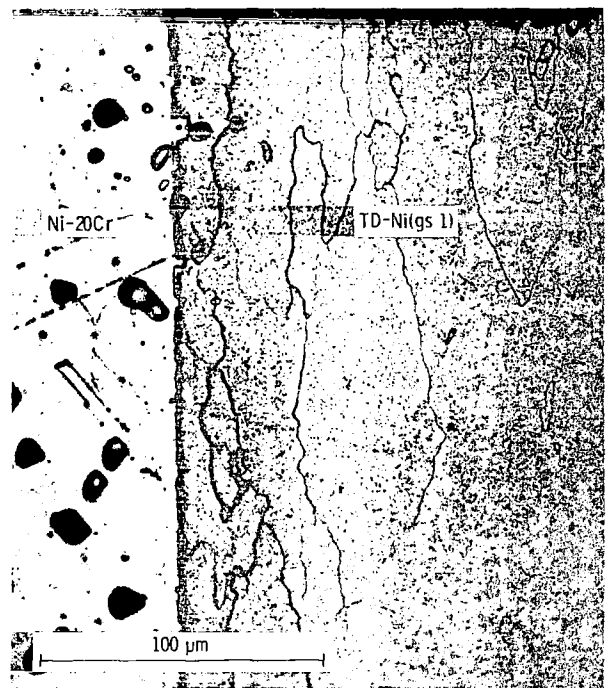
(a) Cr:TD-Ni(gs 1).

(b) Ni-20Cr:TD-Ni(gs 1).
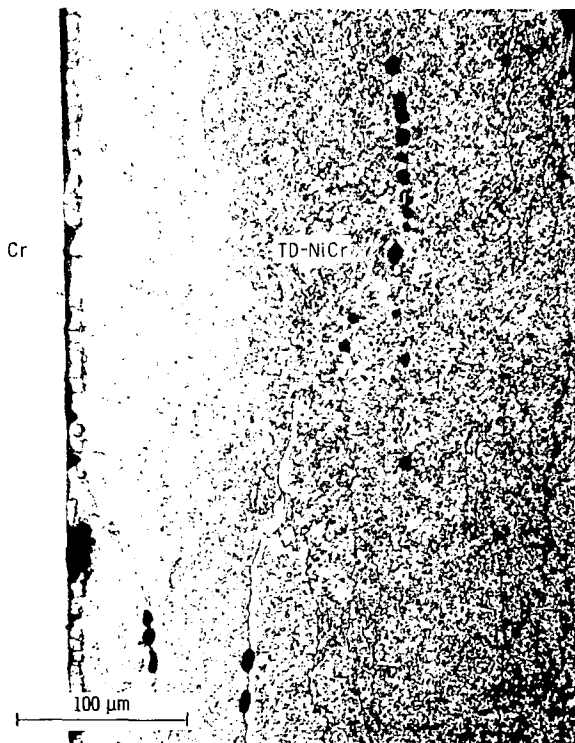
(c) Cr:TD-NiCr.
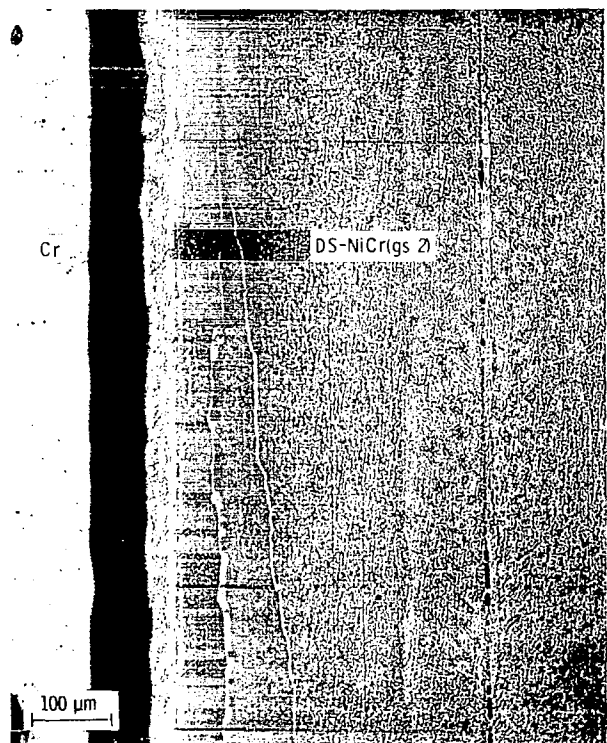
(d) Cr:DS-NiCr(gs 2).

Figure 6. - Photomicrographs of various Cr (alloy):thoriated Ni alloy couples diffused 16 hours at 1260° C in argon. Electrolytically etched with chromic acid mixture.
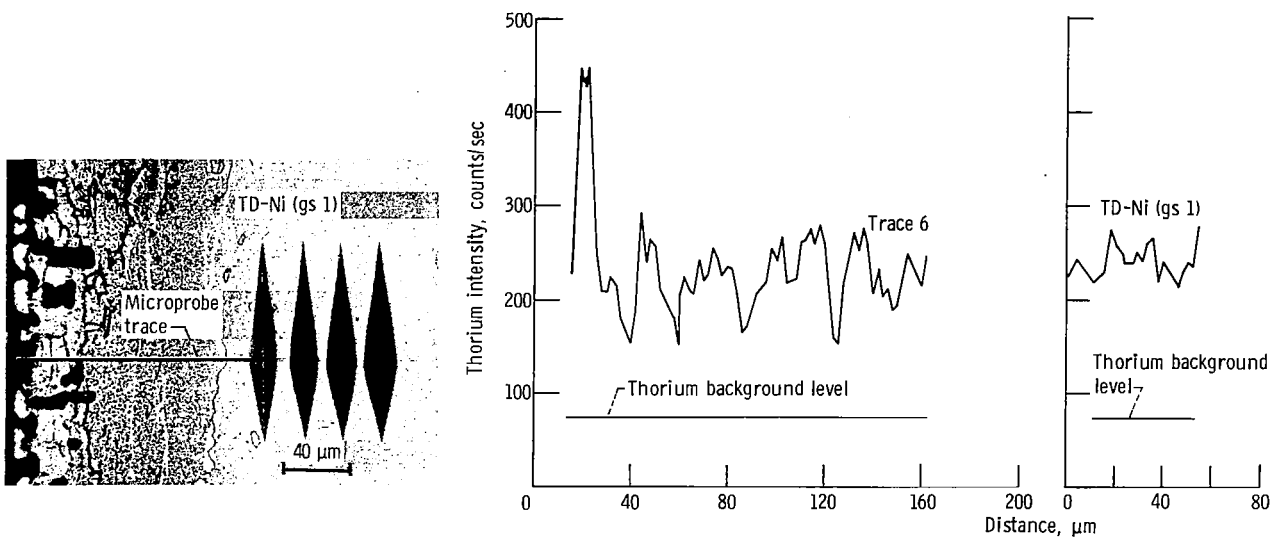
(a) Photomicrograph of region corresponding to trace 6. Electrolytically etched with chromic acid mixture.

(b) Partial thorium profile for trace 6 and TD-Ni (gs 1).
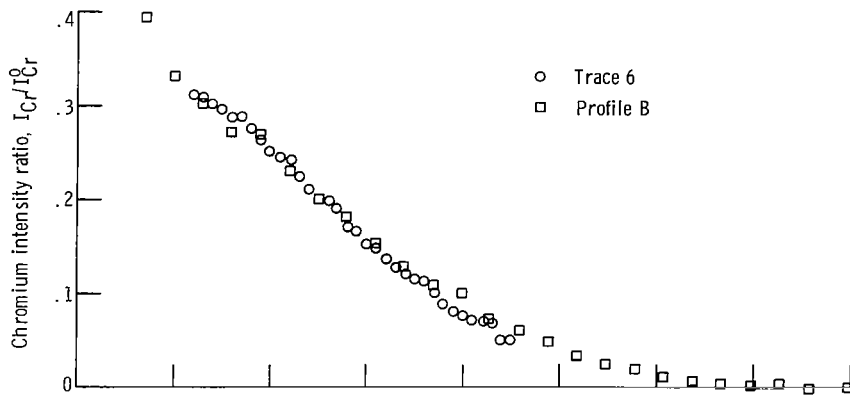
(c) Partial chromium profiles.
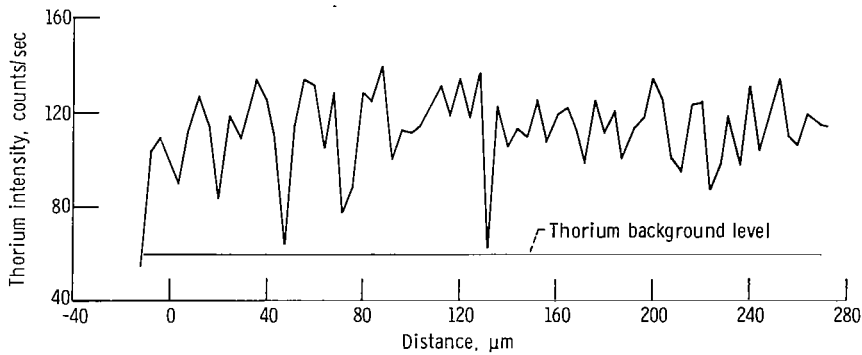
(d) Partial thorium profile for profile B.

Figure 7. – Metallography, thorium profiles, and chromium profiles for Cr:TD-Ni (gs 1) couple diffused 16 hours at 1260° C in argon.
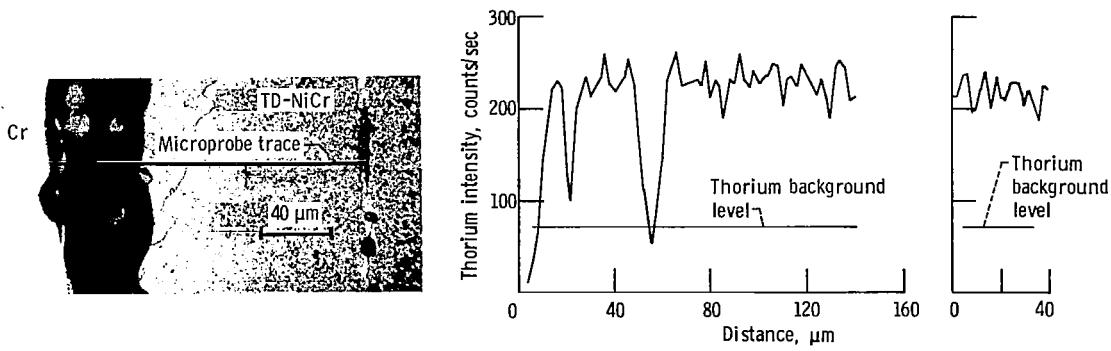
(a) Photomicrograph of region corresponding to trace 11. Electrolytically etched with chromic acid mixture.

(b) Partial thorium profile for trace 11 and TD-NiCr.
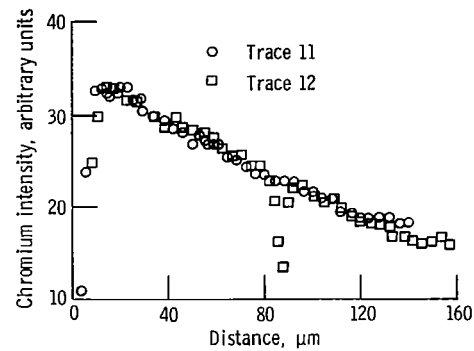
(c) Partial chromium profiles.
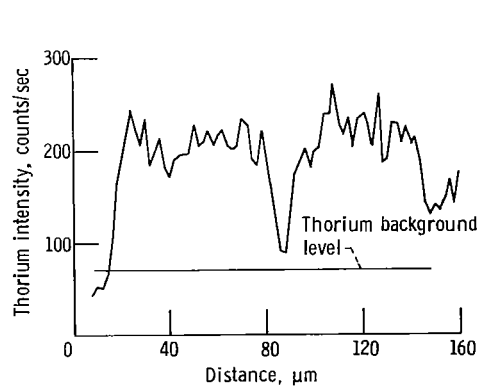
(d) Partial thorium profile for trace 12.
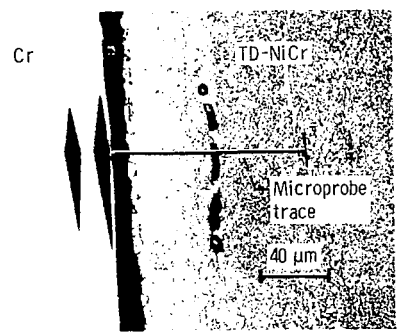
(e) Photomicrograph of region corresponding to trace 12. Electrolytically etched with chromic acid.

Figure 8. - Metallography, thorium profiles, and chromium profiles for Cr:TD-NiCr couple diffused 16 hours at 1260° C in argon.
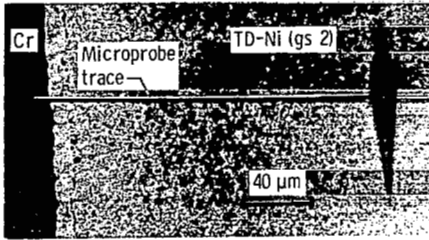
(a) Photomicrograph of region corresponding to trace 9. Electrolytically etched with chromic acid mixture.
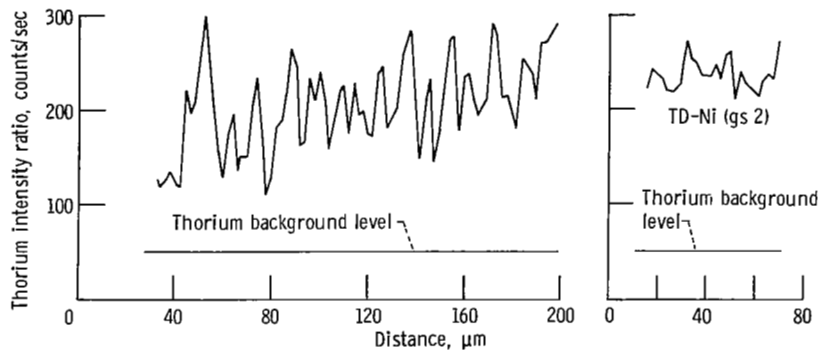


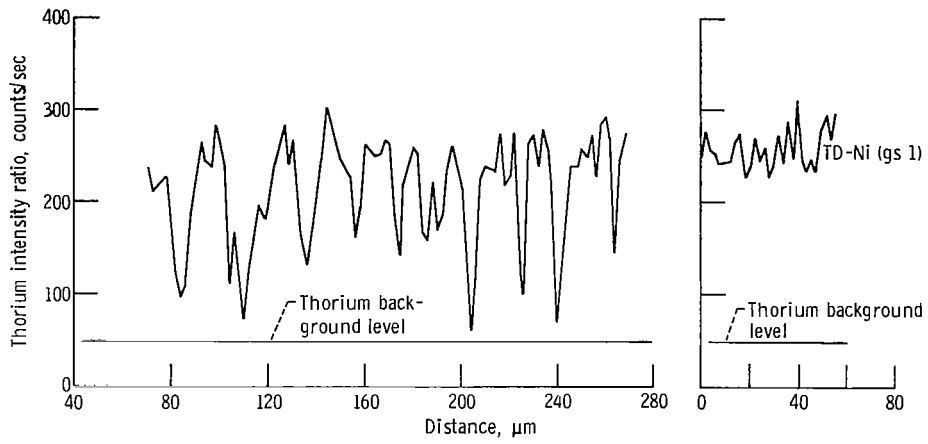(b) Partial thorium profile for trace 9 and TD-Ni (gs 2).
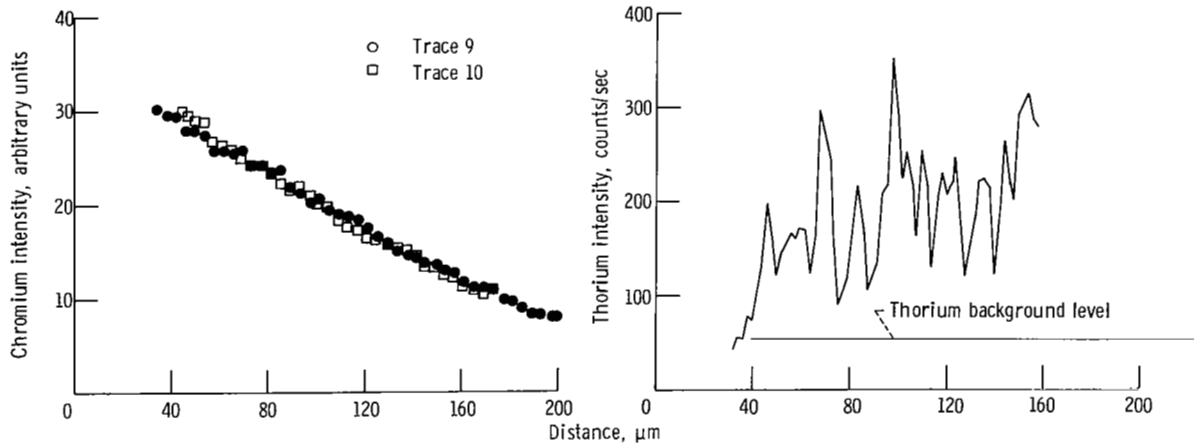


(c) Partial chromium profiles.



(d) Partial thorium profile for trace 10.

Figure 9. – Metallography, thorium. profiles, and chromium profiles for Cr:TD-Ni (gs 2) couple diffused 16 hours at $1260^0$ C in argon.
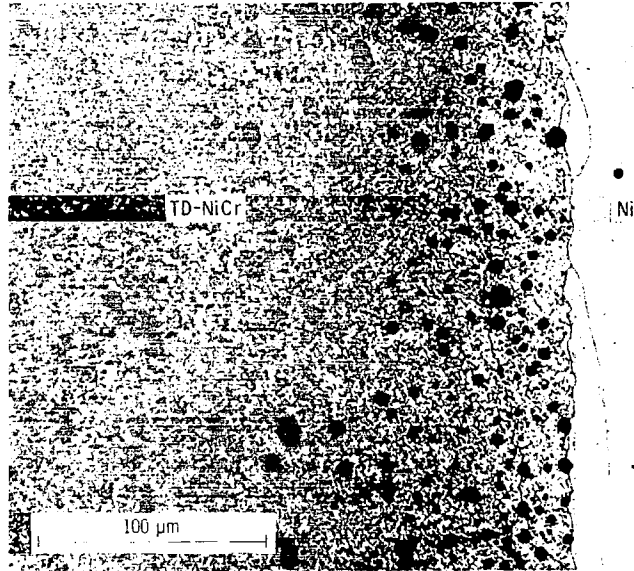
(a) TD-NiCr:Ni. Electrolytically etched with chromic acid mixture.
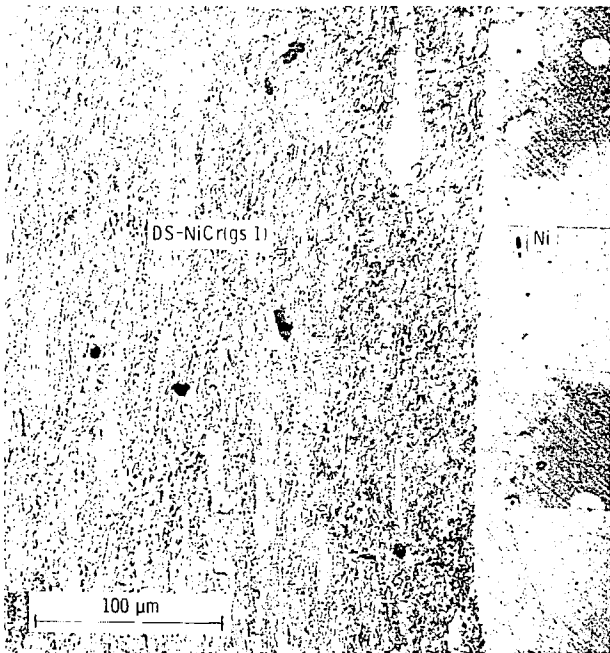


(b) DS-NiCr(gs 1):Ni. Electrolytically etched with buffered aqua regia.
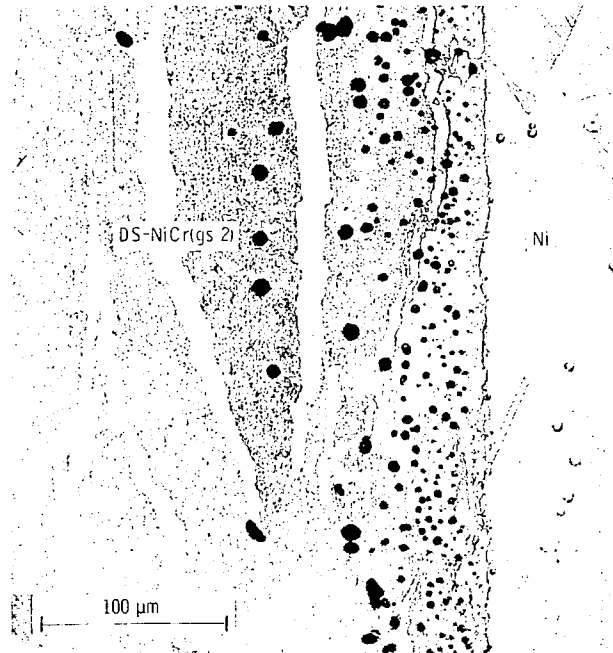


(c) DS-NiCr(gs 2):Ni. Electrolytically etched with buffered aqua regia.

Figure 10. - Metallography, thorium profiles, and chromium profiles for various Ni-20Cr-ThO$_2$:Ni couples diffused 16 hours at 1260$^0$ C in argon.
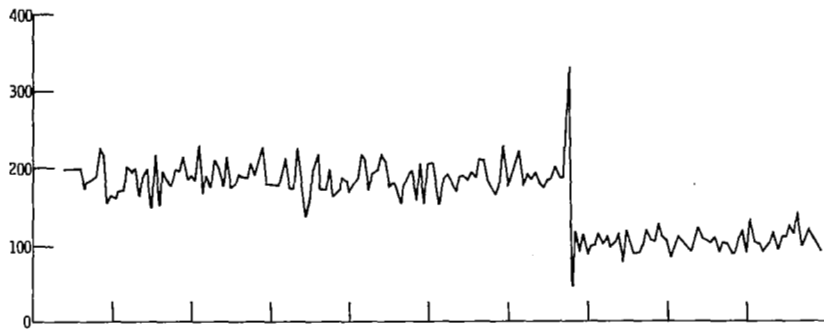
(d) Thorium profile for TD-NiCr:Ni couple.
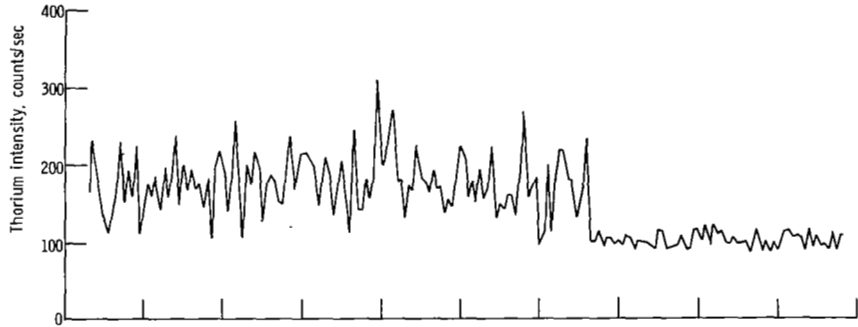
(e) Thorium profile for DS-NiCr (gs 1):Ni couple.
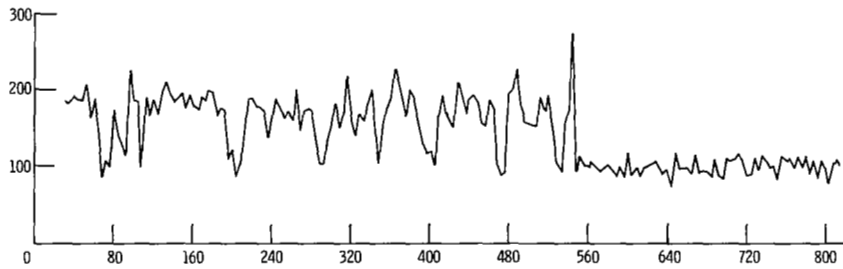
(f) Thorium profile for DS-NiCr (gs 2):Ni couple.
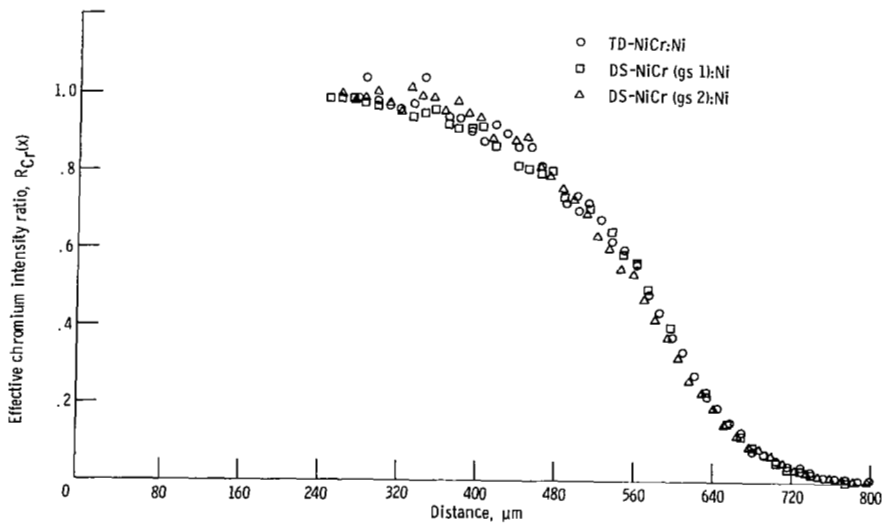
(g) Chromium profiles.

Figure 10. - Concluded.

○   TD-NiCr:Ni
□   DS-NiCr (gs 1):Ni
△   DS-NiCr (gs 2):Ni

30
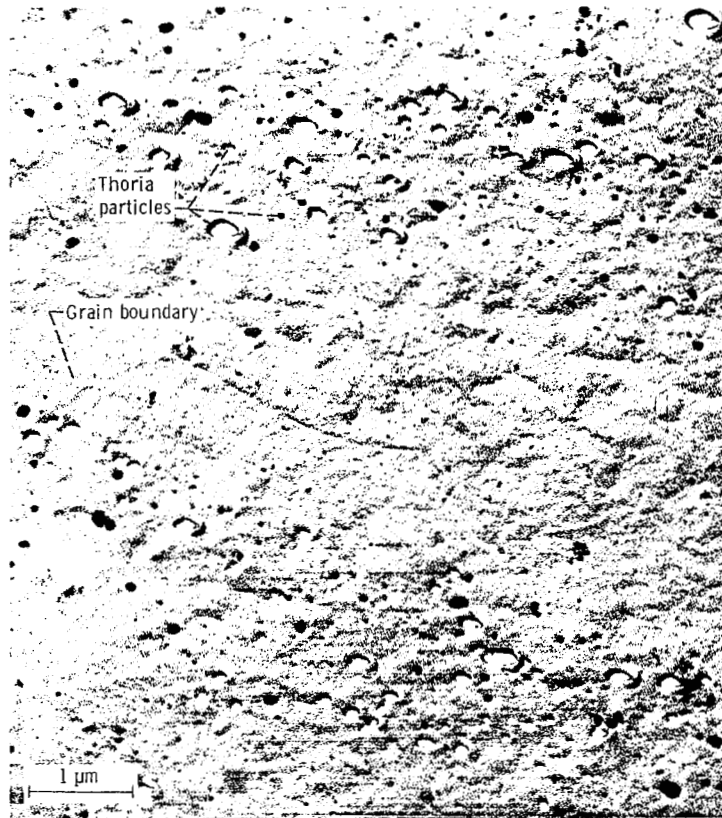
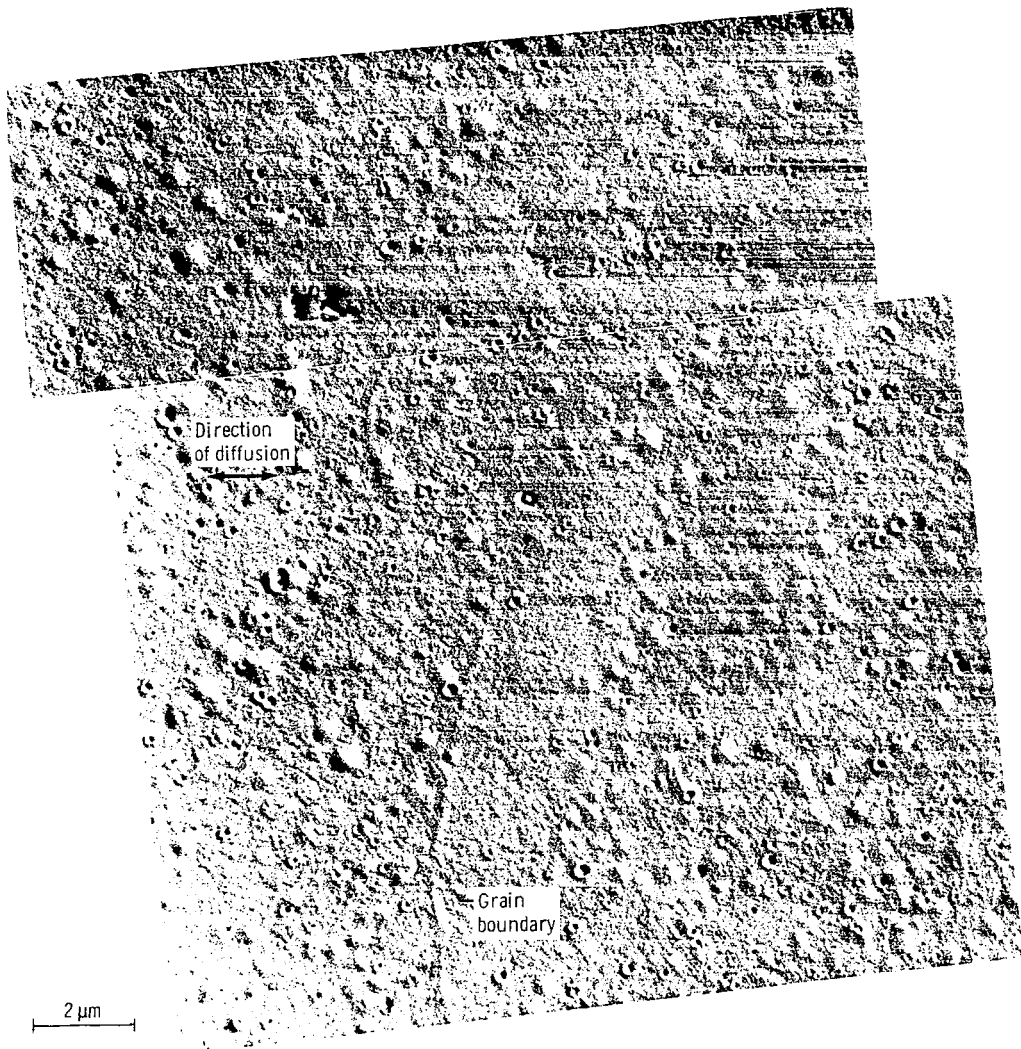Figure 11. – Electron replica photomicrograph of thoria-free band in Cr:TD-Ni(gs 1) diffusion couple.

Thoria particles
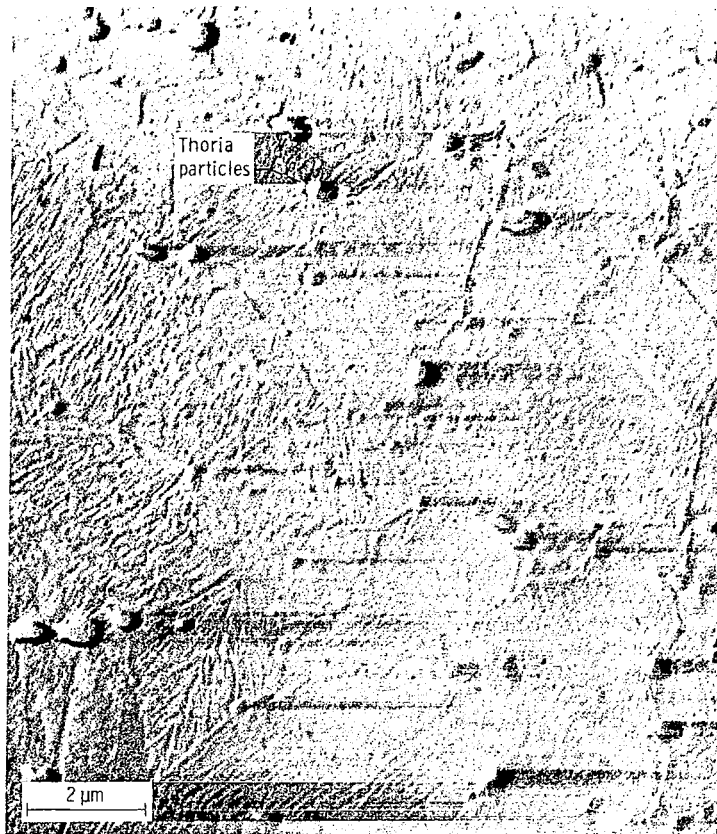
Figure 12. - Electron replica of portion of Cr:TD-Ni(gs 2) diffusion couple.
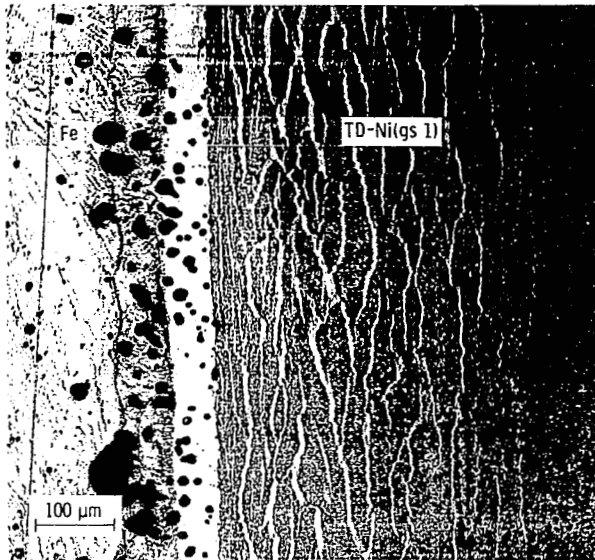
(a) Fe:TD-Ni(gs 1) couple diffused 72 hours. Electrolytically etched
with chromic acid mixture.
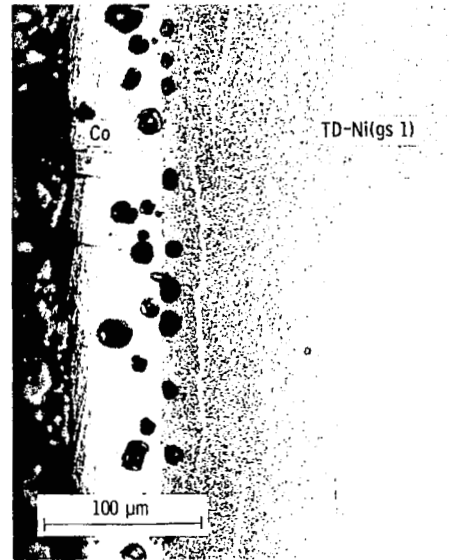
(b) Co:TD-Ni(gs 1) couple diffused 72 hours. Electrolytically etched
with chromic acid mixture.
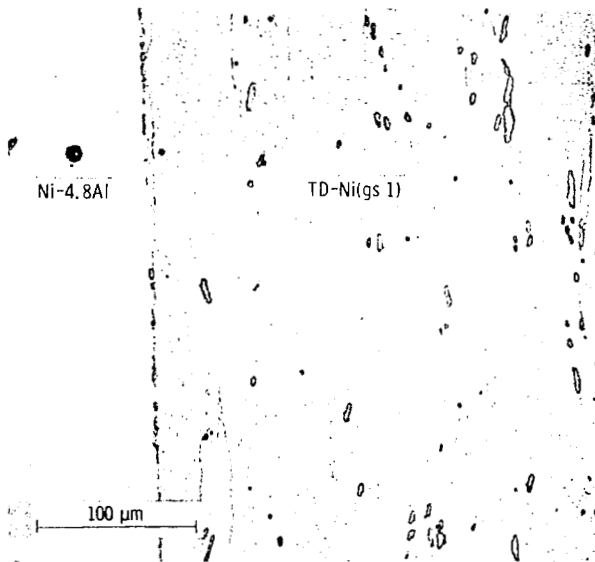
(c) Ni-4.8Al:TD-Ni(gs 1) couple diffused 16 hours. Nickel swab etch
plus chromic acid mixture electrolytic etch.
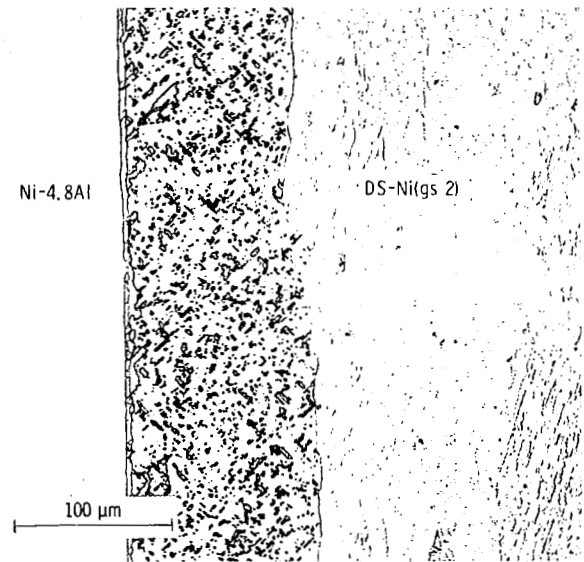
(d) Ni-4.8Al:DS-Ni(gs 2) couple diffused 16 hours. Nickel swab etch
plus chromic acid mixture electrolytic etch.

Figure 13. – Photomicrographs of various alloy:thoriated nickel couples diffused at $1260^{\circ}$ C in argon.
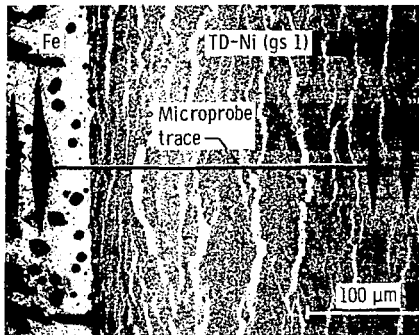
(a) Photomicrograph of region corresponding to trace 19. Electrolytically etched with chromic acid mixture.
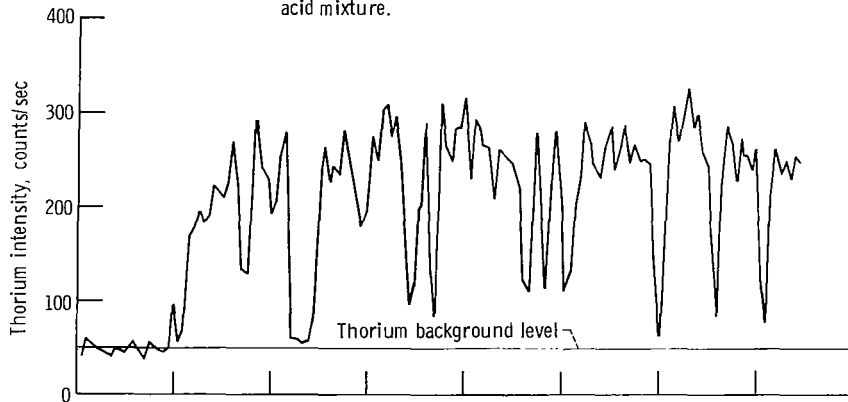


(b) Partial thorium profile for trace 19.
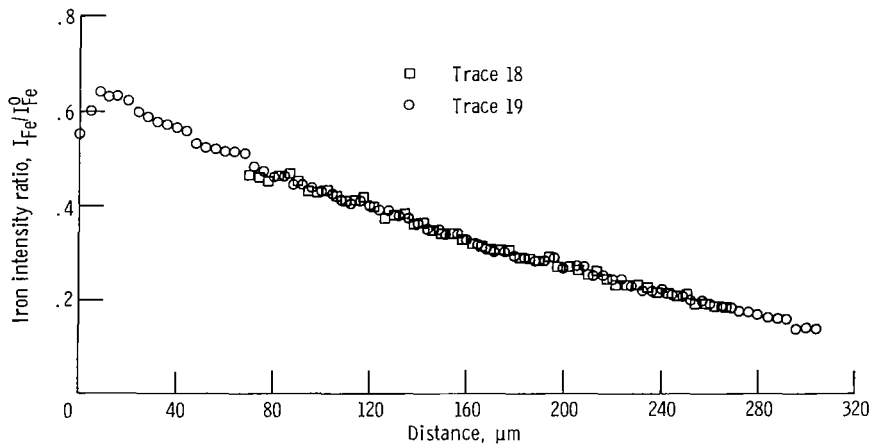


(c) Partial iron profiles.

Figure 14. – Metallography, thorium profiles, and iron profiles for Fe:TD-Ni (gs 1) couple diffused 72 hours at $1260^0$ C in argon.

(d) Partial thorium profile for trace 18 and TD-Ni (gs 1).
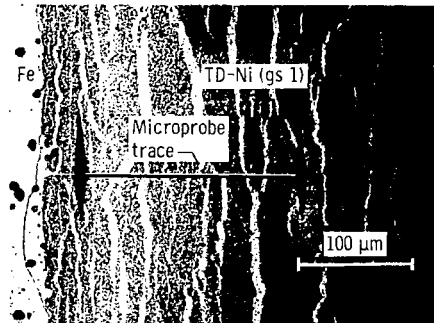


(e) Photomicrograph of region corresponding to trace 18. Electrolytically etched with chromic acid mixture.

Figure 14. - Concluded.
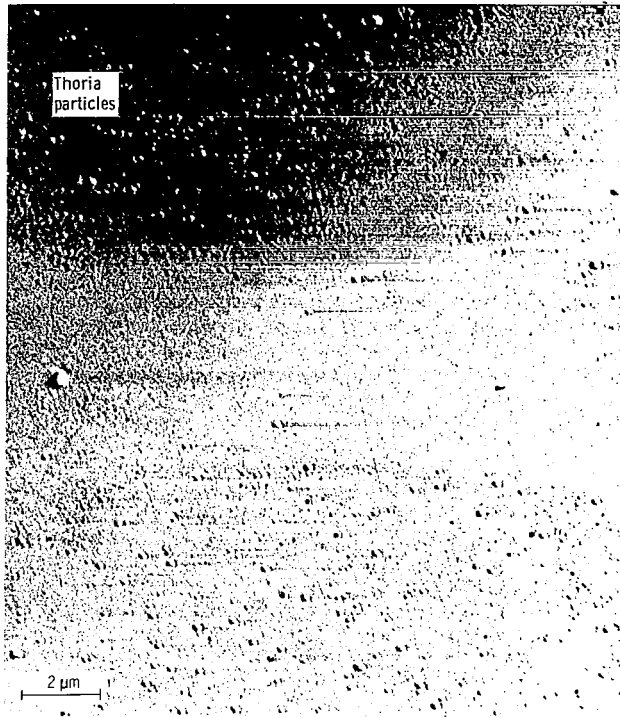
Figure 15. – Electron replica photomicrograph of thoria-free band in Fe:TD-Ni(gs 1) diffusion couple.



(a) Nickel profile (Ni L$_\alpha$ monitered).

(b) Cobalt profile (Co K$_\alpha$ monitered).

(c) Thorium profile (Th M$_\beta$ monitered).
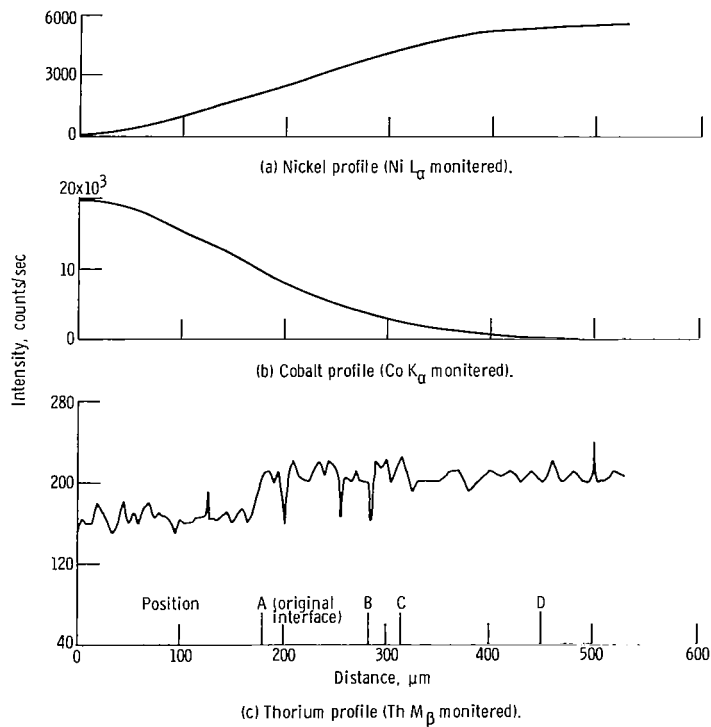
Figure 16. – Continuous electron microprobe traverse of a Co:TD-Ni (gs 1) couple diffused 16 hours at 1260° C in argon.

Grain boundary

Direction of diffusion

2 μm
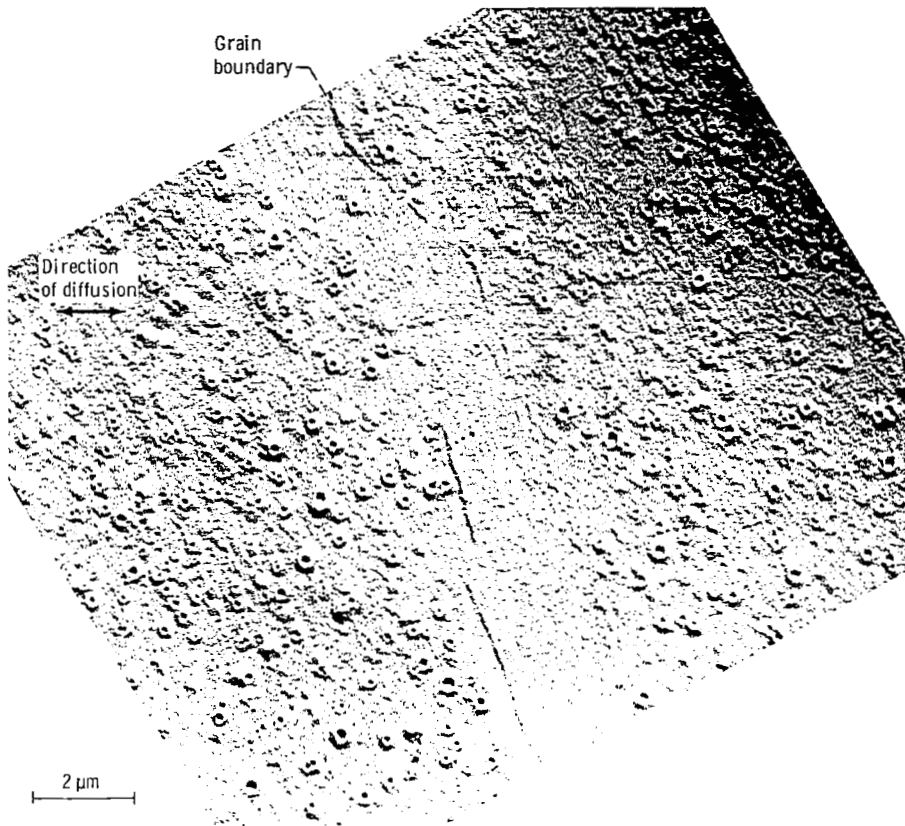
(a) Distance from original interface, ~105 micrometers.

Figure 17. - Electron replica photomicrographs of thoria-free bands formed in Co:TD-Ni(gs 1) diffusion couple.

Direction of diffusion →

Grain boundary

2 μm

(b) Distance from original interface, ~135 micrometers.

Figure 17. - Continued.
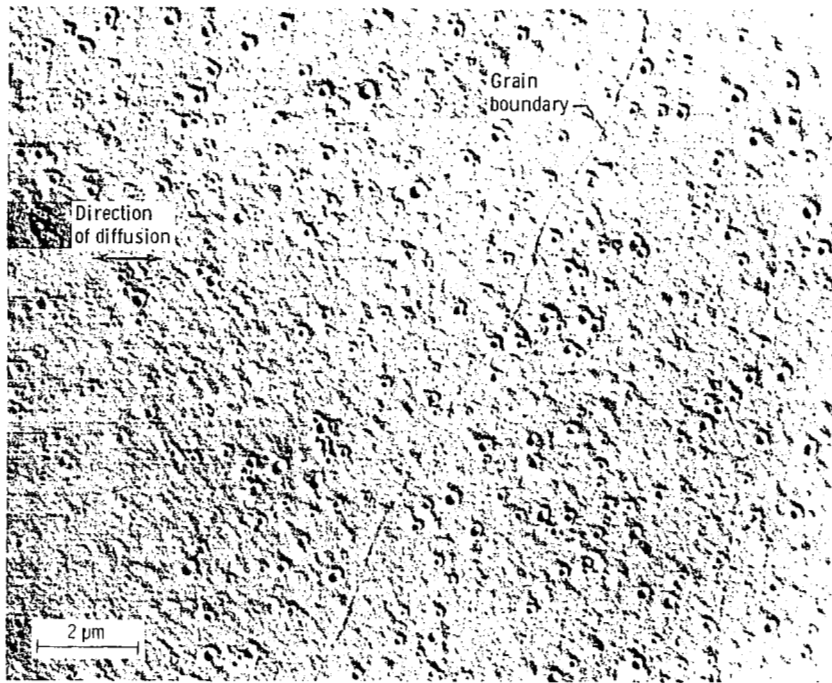
(c) Distance form original interface, ~270 micrometers.
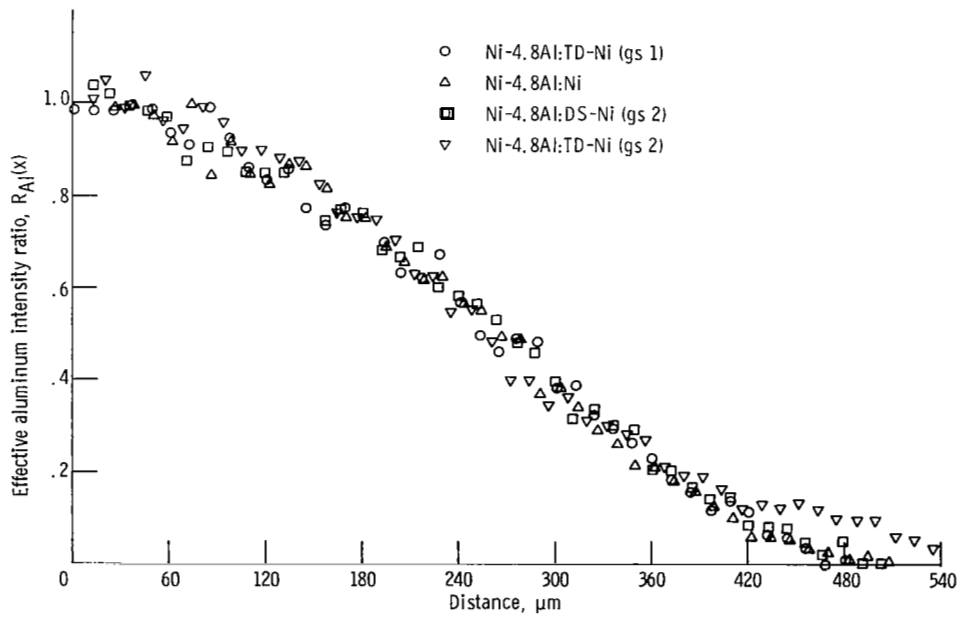
Figure 17. – Concluded.



Figure 18. – Effective aluminum intensity ratio as function of distance for various Ni-4.8Al:Ni diffusion couples. All couples diffused 16 hours at $1260^0$ C in argon.
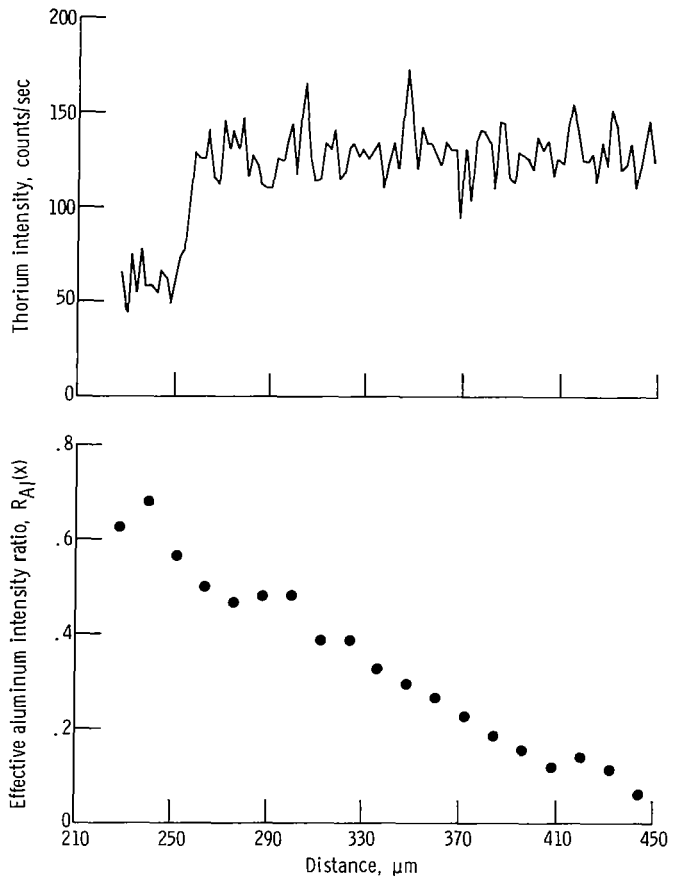
Figure 19. – Partial thorium and aluminum profiles for a Ni-4.8 Al: TD-Ni (gs 1) couple diffused 16 hours at 1260° C in argon.
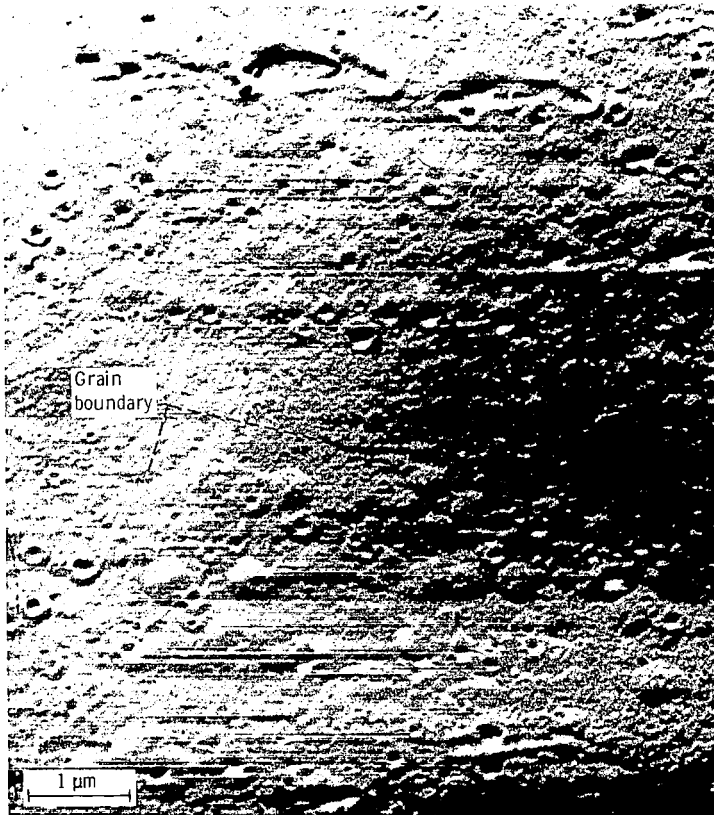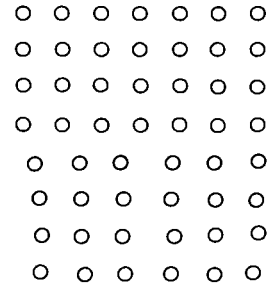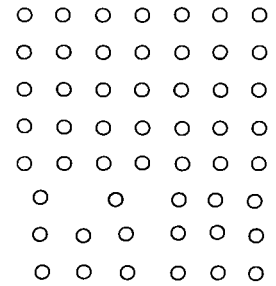
Figure 20. – Electron replica photomicrograph of thoria-free band in Ni-4.8Al:
TD-Ni(gs 1) diffusion couple.



(a) Simple edge dislocation.



(b) Down-climb of edge dis-
location and associated
vacancy.

Figure 21. – The edge dislocation
operating as vacancy source.